Polymers **2010**, *2*, 120-158; doi:10.3390/polym2030120

OPEN ACCESS

polymers

ISSN 2073-4360

www.mdpi.com/journal/polymers

Review

Review on the Functional Determinants and Durability of Shape Memory Polymers

Thorsten Pretsch

BAM Federal Institute for Materials Research and Testing, Division VI.3, 12205 Berlin, Germany; E-Mail: Thorsten.Pretsch@bam.de; Tel.: +49-30-8104-3804; Fax: +49-30-8104-1617

Received: 1 June 2010; in revised form: 5 July 2010 / Accepted: 21 July 2010 / Published: 28 July 2010

Abstract: Shape memory polymers (SMP) belong to the class of stimuli-responsive materials and have generated significant research interest. Their capability to retain an imposed, temporary shape and to recover the initial, permanent shape upon exposure to an external stimulus depends on the "functional determinants", which in simplistic terms, can be divided into structural/morphological and processing/environmental factors. The primary aim of the first part of this review is to reflect the knowledge about these fundamental relationships. In a next step, recent advances in shape memory polymer composites are summarized. In contrast to earlier reviews, studies on the impairment of shape memory properties through various factors, such as aging, compression and hibernation, lubricants, UV light and thermo-mechanical cycling, are extensively reviewed. Apart from summarizing the state-of-the-art in SMP research, recent progress is commented.

Keywords: shape memory polymer; active polymer; shape memory polymer composite; shape memory properties; functionality; degradation; aging; functional determinants; thermo-mechanical testing; durability

1. Introduction

To date, much attention has been directed to a variety of functional materials including alloys [1-3], ceramics [4-6], polymers [7-14] and gels [15-19], which have all been found to exhibit shape memory behavior. Particularly, shape memory polymer (SMP) research is a continuously growing working

field. SMPs have plenty of advantages over their well-investigated counterpart of shape memory alloys (SMAs). Inherent advantages are their low cost, light weight, dyability, corrosion resistance, electrical insulation, ease of processability (formation and workability), adjustable transition temperature and less-demanding thermo-mechanical treatment, also called training. Beyond this, a maximum strain of several hundred percent can be stored by SMPs [20], in contrast to only about 8% by SMAs [7]. SMPs can be biocompatible and nontoxic. Shortcomings of SMPs can be seen in much lower recovery stresses (≤10 MPa [12] *vs.* up to 900 MPa for NiTi [21]), shorter cycle life (200 cycles *vs*. up to 10^6 cycles reported for NiTi [12]), and much longer recovery times (tens of seconds in open air for SMPs *vs*. tens of milliseconds for SMAs [12]). Comprehensive comparisons of SMAs with SMPs have been given by Feninat *et al*. [22] and Hornbogen [23].

An SMP can be deformed from a permanent into a stress-free temporary shape, which can be fixed and maintained until shape recovery is triggered through an external stimulus, most common a temperature increase above the SMP's so-called transformation or switching temperature [7,10,11,24-26]. Depending on the material used, stimuli can also be light [27] (UV [28], infrared or laser light [29-33]), electricity [30,34-44], an alternating magnetic field, pH changes [49] and solvents [50-53].

In Scheme I two different types of SM phenomena and their simplified molecular mechanisms are presented. For classical SMPs with so-called "one-way" (non-reversible) SM, a programming procedure has to be applied every time before the SM effect can be triggered [54]. Similarly, "one-way" triple-shape properties can be obtained by two-step programming of an SMP with two well-separated phase transition temperatures [55,56] or a broad glass transition, spanning, e.g., over a temperature region of 75 °C [57]. Upon application of an external stimulus like heat, the polymer shows sequential shape recovery responses, from twice fixed over once fixed to permanent shape. In some cases, another type of SM phenomenon, which is the so-called "two-way" (reversible, all-round) SM, has been observed. For example, regular temperature-dependent mechanical activity may occur due to crystallization processes, inducing specimen elongation on cooling, and melting transitions, giving specimen shrinkage on heating [58,59]. A detailed mechanism for a glass forming nematic network with reversible SM has been suggested by Qin and Mather [59]. Alternatively, at least five different "two-way" training procedures were published for SMAs [60].

Scheme I. (a) Schematic illustration of the "one-way" SM effect and **(b)** "one-way" triple-shape effect on a polymer specimen (red color) subsequent to shape programming (left). Consideration of the associated molecular mechanisms, illustration of chain segments and netpoints in black and green color (right).

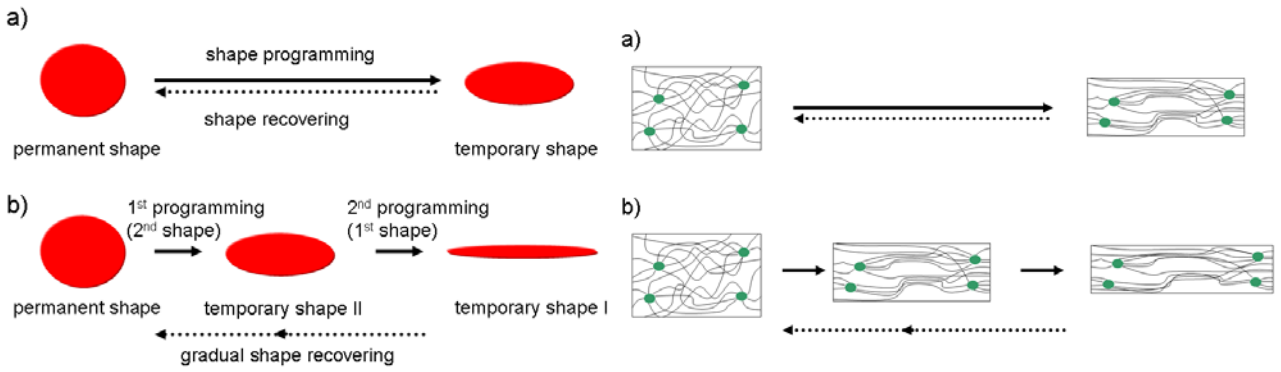

In this article, some fundamental insights on SMPs are provided. In addition, a short overview on polymers with proven SM properties is given and prospects for SMPs are reported. To develop a comprehensive understanding, the relationship between the SM properties of a polymer and the functional determinants, namely structure and morphology on the one hand and processing and environment on the other hand, is elucidated. This is mainly done by giving some series of prominent examples. Beyond this, recent progress in electrically conductive and magnetosensitive SMP composites is reviewed and the alternative triggering of the SM effect in polymers through solvents described. With the summary of durability and cycle life studies on SMPs and their composites, meaningful criterions for the quality of SMPs are considered. Towards the end, two major research trends for SMPs are identified; the first concentrates on medical applications, the other one on foaming. Finally, the focus shifts to impact testing as a powerful tool to evaluate the performance of SMP foams.

2. Fundamentals for SMPs

2.1. Molecular mechanism

Shape memory polymers are polymer networks with integrated, stimuli sensitive switches. Suitable polymer network architectures consist of chain segments and netpoints (Scheme I). Since the netpoints cross-link the chain segments, they determine the permanent shape of the polymer. The cross-links can be either of chemical nature (covalent bonds) or physical nature (intermolecular interactions like crystals and chain entanglements); they prevent flow of the molecular chains under deformation. SMPs can be classified into thermosets and thermoplastics. Thermoset SMPs have chemical cross-links, which soften, but do not melt at elevated temperatures; instead they either start to burn or decompose. In general, thermoset SMPs have higher stiffness and lower strain capability than thermoplastic SMPs, which are easy to reshape, since they have no covalent bonds between chains (no chemical cross-links) [20]. Physical cross-linking is commonly found in block copolymers, whose morphologies consist of at least two segregated domains. In such examples, domains related to the phase with the highest thermal transition temperature (T_{perm}) are called "hard domains" and act as physical netpoints [7], they aggregate to form permanent netpoints through polar interactions, hydrogen bonding and crystallization [61]. The hard segments constitute the permanent shape of an SMP, but to obtain SM functionality a second phase is required. The chain segments associated with the second highest thermal transition temperature (T_{trans}) are called "switching segments" and form a reversible phase, which can be first used for fixing a temporary shape in an SMP through polymer chain immobilization (crystallization or vitrification) and later to accomplish molecular motions during shape or stress recovering due to passing a melting ($T_{trans} = T_m$) or glass transition ($T_{trans} = T_g$). Chemical cross-linking is achieved by the reaction of functional groups, which are attached to chain segments. The functional groups must be able to reversibly form covalent bonds by reacting with each other.

The mechanical properties of polymers differ greatly depending on the region of viscoelastic behavior [62]. An abrupt drop in tensile modulus E_r by a factor of more than 100 during polymer heating from a temperature below to above its phase transition is a well-known phenomenon, which can be observed in many polymers. Scientists and engineers have learned to take advantage of the

pronounced change in E_r through the application of suitable programming steps around the phase transition, which provide regular polymers with shape memory characteristics [54]. An SMP can be deformed with relative ease at temperatures above the phase transition and fixed by cooling below the phase transition temperature. Accordingly, the rubbery modulus dictates the recovery force of an SMP [63], it is the basis of the SM effect in polymers and scales with the strain capacity of such materials [64]. E_r is known to be inversely proportional to the molecular weight between cross-links, according to James' classical work on the elastic theory of rubber [65]. In segregated shape memory polyurethanes (SMPUs), the sharpness of the glass transition is dependent on the degree of phase mixing; an increase in phase mixing normally results in the broadening of a glass transition. Factors that control the degree of phase separation include copolymer composition, block length (molecular weight), crystallinity of segments, synthesis conditions and thermal history [66-68].

One fundamental prerequisite of SM behavior is the successful application of shape programming, during which the flexible switching segments of an SMP are elongated along the deformation direction before the stretched polymer is fixed under stress in its temporary shape through crystallization or vitrification. At the molecular level, staying above the shape fixing temperature would lead to relaxation of an applied strain, if the polymer is unloaded at that temperature, due to structural recoil of the switching segments as soon as stress is released according to normal rubber elasticity [23]. When activated after programming, either strain or stress recovery results from the relaxation of temporarily "fixed" polymer chains, which can be ascribed to the phenomenon of entropy elasticity. Thus, the polymer restores its random coil conformation [69]. As consistent with Flory's theory [70], the primary driving force for the SM effect is the low conformational entropy states created and frozen during shape programming [71]; it is energetically favorable for the polymer chains to finally return to their most disordered conformation [13].

2.2. Examples

The list of polymers with SM properties is continuously growing; it includes physically [72-78] and chemically [79-81] cross-linked SMPUs, trans-polyisoprene-based SMPU [82,83], poly(ether ester)s like poly(ethylene oxide)/poly(ethylene terephthalate) copolymers [84-86], norbornyl/polyhedral oligomeric silsesquioxane (POSS) copolymers [87,88], poly(methylene-1,3-cyclopentane) and its copolymer with polyethylene [89], styrene/butadiene copolymers [90], thiol-ene/acrylate copolymers [91], polynorbornene [90], polymer networks prepared from poly(ε-caprolactone) (PCL) dimethacrylates [92,93], acrylate-based SMPs [94], (meth)acrylate networks [95,96], cross-linked polyethylene [97], epoxy-based polymers [98-101] and many others. Moreover, various polymer blends like SMPU/phenoxy resin [102], SMPU/polyvinylchloride (PVC) [103] and several others [104-109] have received attention. Inspired by the potential to combine blending and post cross-linking, scientists developed SMPs with interpenetrating polymer network (IPN) structures [110]. Extensive overviews on SMP research have been given by Lendlein and Kelch [7], Liu *et al*. [10], Ratna and Karger-Kocsis [11], Rousseau [12], Meng and Hu [43] and Mather *et al*. [13]. In these works, the different types of SMPs were classified according to their chemical architecture, the type of transition temperature (T_g/T_m) and the associated shape recovering mechanism, and the type of cross-linking (chemically/physically). Beyond this, the relevant structure-property relationships were summarized.

2.3. Applications

According to any envisioned application, requirements like polymer structure and morphology have to be adapted and combined with additional processing and programming technology [7]. Due to their unique characteristics and great potential, SMPs have been considered for various applications [111], including morphing aircraft [112-117], clothing manufacturing [118-123], adhesives [124,125], water-vapor permeability materials [126,127], mandrels [128-130], self-deployable structures [131-135], end-of-life cycle applications [136-138], structural repair, additives for cementitious materials [139], artificial muscles [140,141], micron-sized actuators [142], Braille paper [111], adhesives [143,144], pharmaceutical applications [145], orthodontic applications [146,147], medical treatment [147-149] and eye-glass frames [150]. However, the realization of novel concepts requires in-depth knowledge of shape programming and the optimization of shape recovery behavior according to operational demands. Apart from the employed trigger method (Section 1) the polymer's response time, for instance, plays a crucial role. It is restricted by several factors, e.g., the trigger mechanism, the SMP's thermal conductivity, transition temperature and its dimensioning. Beyond this, the understanding and alleviation of degradation phenomena, which may significantly alter an SMP's thermo-mechanical behavior, is a prerequisite for the successful implementation of this promising technology.

3. Functional Determinants

3.1. Structure and morphology as functional determinants

The SM effect in polymers originates from the existence of a thermally "reversible" phase transition, e.g., from glassy to rubbery state, and from distinct phase separation among hard and soft segments due to the incompatible nature of each segment [151]. As known from thermoplastic block copolymers like SMPUs, such interactions among hard segments, like hydrogen bonding, dipole-dipole and induced dipole-dipole interactions, have a significant impact on the phase separation of hard and soft segments, same as the ratio of crystalline to amorphous domains and presumably the size distribution of crystallites. In terms of SM properties, shape retention is known to derive from the interaction between hard segments, which form well dispersed domains (frozen phase) within the soft segment matrix. The latter is the reversible phase and accounts for the material's shape recovery behavior due to the reversibility of phase transition [152]. The synthesis route (e.g., the ratio of hard to soft segments) and the polymerization procedure directly impact SM properties and the polymer's crystallinity with respect to domain size distribution, ordering, grain size and symmetry [73,74,153]. Hereafter, some notable developments in the area of SMPUs are reviewed. In particular, recent attempts that seek to understand structure-property relationships and aim at characterizing morphological influences are highlighted.

For a deeper understanding of the microphase morphology of (PCL/1,4-butanediol (BDO)/hexamethylenediisocyanate (HDI))-based SMPU, D'hollander *et al*. [154] utilized solid-state proton wide-line nuclear magnetic resonance (NMR) relaxometry, combined with synchrotron small-angle (SAXS) and wide angle (WAXD) X-ray scattering. The authors found a conversion from dispersed, randomly placed hard segment domains into progressively more periodic and interconnected

hard segment nanophases with increasing hard segment content from 12 to 35 wt% and that higher cooling rates favored the formation of finer phase morphologies.

Cho *et al*. [151] took advantage of pentaerythritol as a four-way cross-linker for SMPU block copolymers. For the investigated (polytetramethylene glycol (PTMG)/4,4'-methylene bis(phenylisocyanate) (MDI))-based SMP, it was shown that the chemical cross-linking of hard segments through pentaerythritol, using different cross-linker contents of 2, 4 and 6 wt% at hard segment contents of 25 and 30 wt%, respectively, gives best SM properties at hard segment contents of 25 wt% and the highest cross-linker contents chosen. Here, shape fixity ratios of 91% and shape recovery ratios of 94% were held after the third thermo-mechanical cycle for maximum strains of ε_m = 100%. Interestingly, the increase in hard segment content by 5 wt%, while simultaneously keeping the cross-linker content constant, favored drops in shape fixity close to 50% and in shape recoverability to 70%. This finding illustrates that the identification of the optimum hard to soft segment ratio and cross-linker content is of major importance to maximize the SM properties of a polymer. The difficulty is mostly due to the fact, that there is no linear relationship between the mentioned parameters. Studying semicrystalline thermoplastic (PCL/MDI/BDO)-based SMP with varying soft segment length (1,600–7,000) and hard segment content (7.8–27%), Li *et al*. [74] discovered that specimens with short soft segment length (low number average molecular weight of 1,600) and high hard segment content of 37 wt% exhibited extremely weak shape recovery ratios close to 20%, whereas specimens with much higher soft segment molecular weight of 7,000 and lower hard segment content of 19 wt% displayed shape recoverabilities close to 100%. The authors also reported that when hard segment contents fell below a critical barrier of 10 wt%, the hard segment domains were no longer able to serve their function as physical cross-links at temperatures above the melting temperature of PCL. Further insights on the functional determinants came from Kim *et al*. [155], who conducted a systematic study on the effect of soft segment content and its molecular weight on PU ionomers and the corresponding non-ionomers. They demonstrated for (PCL/MDI/BDO/dimethylolpropionic acid (DMPA))-based SMP that phase separation was enforced through the introduction of additional intermolecular interactions within hard domains, which had the effect to increase hard domain cohesions and in addition storage moduli, both in the glassy and rubbery state. In conjunction, the ionomer gave better shape recoverability compared to the non-ionomer, as mainly associated with the increase in rubbery state modulus of the ionomer. Similar polymer systems were studied by Jeong *et al*. [156], whose results revealed a reduction in functional fatigue through the incorporation of ionic moieties into hard segments. Aside from the advantageous cyclic thermo-mechanical properties, the additional benefit, which can derive from SMPU ionomers, is antibacterial activity [157,158].

Chen *et al*. [159] focussed on the modification of phase separation between hard and soft segments in poly(1,4-butylene adipate) glycol (PBAG)-based and poly(hexamethylene adipate) glycol (PHAG)-based SMP. For this purpose, the low-molecular-weight lubricant 1-octadecanol (ODO) was added in the manufacturing process to end-cap PU chains via a urethane reaction between isocyanate-capped PU prepolymers and hydroxyl groups of ODO. In another approach, liquid paraffin (LP) was used as outer lubricant. The unveiled concept turned out to be successful, since the promotion of phase separation through the lubricants was indicated and SM properties could be improved. Most strikingly, a clear enhancement in shape fixity from 85 to 100% for specimens

containing 0.3 wt% ODO could be detected. It was also found that the strain recovery temperature increased by more than 6 °C for systems containing 0.6 wt% of ODO and by 4.5 °C for those with 5 wt% of LP.

Cao and Liu [160] followed the approach of soft segmental SMPU hyperbranching. Hyperbranched polymers are a special type of dendritic polymers with densely branched structures and a large number of reactive groups. The associated monomers with mixed reactivities, commonly denoted A_2B or A_3B, resemble each other in both end-group functionalities and molecular weights and align through polymerization, thus giving branched structures with exponential growth [161,162]. In the given case, the hard to soft segment relationship in (Boltorn®H30/PBAG/MDI)-based SMP ($T_{trans} = T_m$) was dominated by a general trend of decreasing soft segment crystallinity with increasing hard segment content. Almost complete shape recoverabilities of 96 to 98% and thus the best SM properties could be witnessed for hard segment contents of 15–35%. Here, the shape fixity ratio decreased from 94 to about 90% with increasing hard segment content, which was explained by an increase in polymer rigidity. The SM effect was triggered in an oil bath with a hot stage on programmed specimens (ε_m = 300%). In an $A_2 + B_3$ approach, Sivakumar and Nasar [163] used PCL/PU oligomers as A_2 monomers and trifunctional alcohols as B_3 monomers, from which biocompatible, hyperbranched SMPU could be synthesized. It was found that the branching density had no effect on the crystallizability of the investigated hyperbranched polymers, so that the SM characteristics remained nearly unaffected. However, the shape recovery speed could be significantly shortened as substantiated by dynamic mechanical analysis (DMA), which revealed an increase in the storage modulus *E*' for hyperbranched SMPU.

In summary, from the abovementioned studies, it can be concluded that gaining a deeper understanding of the main structure-property relationships in SMPs is eminent for the development of new SMPs with superior functional properties and should therefore be a desirable goal in the future.

3.2. Processing and environment as functional determinants

Polymer processing conditions and technique may strongly influence the mechanical and SM properties of a polymer. In principle, SMPs can be formed into an initial, permanent shape by conventional processing methods, e.g., injection molding [164]. Zeng and Zhang [165], for example, studied the effect of varying reaction and curing temperatures on the morphology and mechanical properties of ester-based SMPU. The authors witnessed lower soft segment crystallinity with increasing reaction temperature (from 90 to 100 °C) and curing temperature (>60 °C). In one case, the raise of curing temperature from 18 to 80 °C led to an increase in tensile strength from 6 to 16 MPa and in elongation-at-break from 41 to 822%, suggesting a strong increase in cross-linking density. The given insights were confirmed by similar studies conducted by the same authors [166] on ester-based SMPU blended with chitosan. Although not reported, it is most likely that significant changes in processing go along with the substantial modification of SM properties. In contrast, contributions in the textile area, which is a highly promising field for novel SMP applications [120,122], also focussed on the impairment of SM properties through processing. One nice example was given by Hu *et al*. [167], who investigated the influence of the processing temperature on the microstructure and thermo-mechanical properties of an SMPU from Mitsubishi Heavy Industries (MHI). In a first step,

different SMPU membranes were prepared by solution casting at 70, 120 and 150 °C. The films casted at higher temperatures gave rise to high hard segment crystallinity, more apparent phase separation and better water-vapor permeability. The SM properties were compared in bending tests; the best shape recoverabilities were obtained for samples casted at 120 °C. Taking another step forward, the same group [168] elaborated a concept of SMPU wet spinning. They synthesized a set of (poly(ethylene adipate) glycol (PEAG)/MDI/BDO)-based SMPUs through copolymerization in *N*,*N*-dimethylformamide (DMF). The SMPUs were wet spun into fibers and thin films prepared as standard for comparison. It was found that the fibers showed less pronounced shape fixities, but better shape recoverabilities than the films. In general, a clear enhancement in recovery stresses through wet spinning was observed; in one of their examples even an increase from approximately 3.3 to 11.0 MPa. In another work [121], the group focussed on the comparison of wet and melt spinning technologies for SMPU fibers. Compared to wet-spun fibers, the melt-spun fibers had higher tenacity and breaking strains and revealed superior shape fixity and recovery ratios. The results indicated higher phase separation for melt-spun fibers, allowing for better hard and soft segment crystallization, whereas the wet spinning technology seemed to hinder the formation of well-organized hard and soft segments. Accordingly, the authors concluded that the melt spinning method was superior to wet spinning. In a further contribution [169], the group reported on the fabrication of electrospun PCL-based SMPU fibers of ultrafine diameters between 50 and 700 nm. The nanofibers showed good SM properties as evidenced by cyclic tensile tests. In detail, shape recoverabilities of 98% and shape fixities of 80% could be detected. Ultrafine fibers provide unexpected high surface area to volume ratios and are of interest for many applications, ranging from textile to composite reinforcement, sensors, biomaterials and membrane technology [170]. Apart from that, it is worth mentioning that the temperature dependency of water-vapor permeability (WVP) is an important criterion, which has to be taken into account for the effective utilization of polymers in water-proof textiles [171,172]. Jeong *et al*. [173] discovered that better WVP can be obtained for thermoplastic SMPUs with lower T_g values. The authors successfully employed hydrophilic segments such as DMPA in order to enhance the WVP. The observed increase in WVP was attributed to an improvement of chain mobility when passing the phase transition. In this connection, further extensive studies on physical properties with regard to air permeability, thermal expansion, *etc*. would be desirable. However, a nice summary of the state-of-the-art in stimuli-responsive polymer research with the focus being on textile applications was given by Hu *et al*. [123].

Finally, the last functional determinant to be introduced is the “Environment”. To date, literature focuses on the functional study of SMPs in a laboratory environment (thermochamber, water bath, *etc*.). In this way, the environment, which is used to evaluate SM properties, is equalized with the utilized thermo-mechanical characterization method. Applications for SMPs are diverse and involve deformations like bending, compression and drawing, accordingly there are different testing methods to quantify the SM behavior of a polymer, such as bending tests [174-176], fold-deploy tests [135], uniaxial experiments (unconstrained free strain recovery tests, stress recovery tests under full constraint at a fixed strain level [101,177], isothermal uniaxial compression tests [178] and other tests developed for SMP foams [179-183]) and isothermal free strain recovery tests in warm water baths, during which a video camera collects images at a well-defined rate, e.g., at 20 frames-per-second (Figure 1) [184,185]. In some cases, a dynamic mechanical analyzer has been used to evaluate SM properties [88].

Figure 1. Shape recovery of coiled poly(lactic acid)/poly(vinyl acetate) (30:70) blend upon exposure to a water bath (65 °C). Reprinted with permission from [185]. (© 2003, Society of Plastics Engineers).

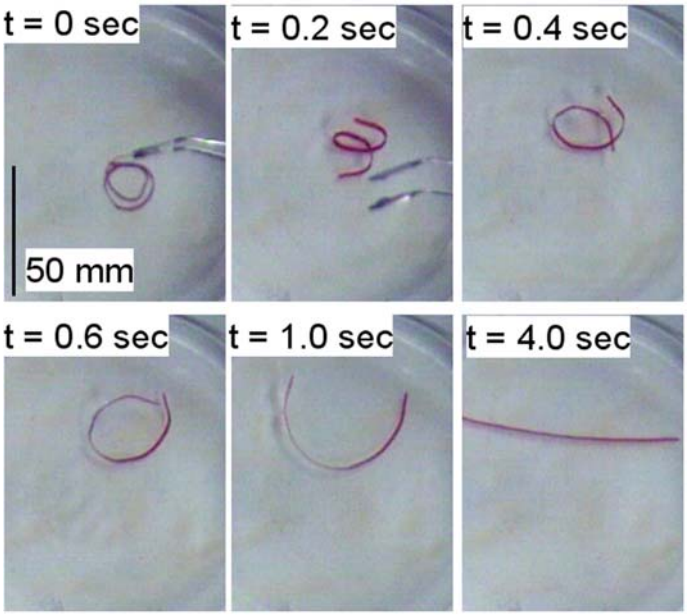

Commonly, functional performance testing is done by using a tensile testing machine equipped with a thermochamber. Cyclic thermo-mechanical measurements (CTMs) often consist of four distinct steps:

1 Polymer deformation at $T_{high} > T_g$ or T_m (T_m = soft segmental melting temperature);
2 Shape fixing at constant strain by cooling to $T_{low} < T_g$ or T_c (T_c = soft segmental crystallization temperature);
3 Unloading at a temperature below the shape recovery temperature, e.g., at $T_{low} < T_{trans}$ with $T_{trans} = T_g$ or T_m, in order to determine the amount of fixed strain;
4 Heating above the shape recovery temperature T_{trans} in order to either induce strain (free strain recovery without any external constraint) or stress (stress recovery in the presence of fixed strain constraint) recovery responses.

Accordingly, the first three steps involve the programming of an SMP, the last one the specimen recovery. From a series of N CTMs, a data set can be obtained, which allows e.g., to determine the strain fixing ability (shape fixity ratio R_f) and strain recoverability (shape recovery ratio R_r or total shape recovery ratio $R_{r,tot}$) of a tested SMP [7], or to quantify the recovery stresses. The recovery behavior is strongly influenced by the amount of stress applied to the polymer and by its thermal expansion behavior [101,186,187].

The cyclic thermo-mechanical behavior of an SMP depends on the polymer's thermal and visco-elastic properties (e.g., the thermal transition temperatures, broadness of the transitions, expansion behavior, intensity of change in modulus), specimen size, clamping conditions (gauge length and clamping pressure), load cell sensitivity (setting of proportional-integral-derivative parameters) and testing conditions (deformation temperature and rate, maximum strain, temperatures T_{high} and T_{low}, holding times, heating/cooling rates, number of testing cycles) [71,177,187,188]. Before testing, all these parameters have to be carefully selected in accordance with the material's mechanical

properties. From a polymer testing expert's viewpoint, the variety of possible settings is both a blessing and a curse. Although detailed settings can be made to meet the optimum testing conditions for an SMP, it becomes more and more difficult to compare different scientific data sets with each other, unless exactly the same way of testing has been chosen.

Some relevant contributions in the field of SMP testing came, inter alia, from researchers around Gall [99], who reported for epoxy-based SMP ($T_{trans} = T_g$) that the choice of deformation temperature, which has also been termed "pre-deformation temperature" [188], influences the SM behavior. Polymers, which were deformed at $T_d > T_g$, revealed an increase in recoverable stress for larger amounts of fixed strain. The same group [71] also observed for acrylate-based SMP ($T_{trans} = T_g$) that lower deformation temperatures ($T_d < T_g$) decrease the temperature required for free strain recovery and favor much higher recovery stresses. This phenomenon is explicable with the fact that polymer chains can relax when deformed at temperatures well above T_g, but not below. Beyond this, it could be observed that the stress recovery paths changed under full strain constraint from sigmoidal to "peak-containing", when T_d was lowered from above to below T_g. Further insights came from Miaudet *et al*. [189], who reported on the so-called "temperature memory effect" (TME), which means that a stress recovery peak under constrained conditions was observed at that temperature, where a polymer had been initially deformed, as evidenced for composites made from poly(vinyl alcohol) (PVA) and carbon nanotubes (CNTs). In a recently published work from Xie [57], the author revealed that in the broad glass transition region of perfluorosulfonic acid ionomer (in between 55 and 130 °C) the polymer was capable of memorizing T_d. Moreover, the author indicated the adjustability of recovery stress just through the proper choice of deformation temperature and reported on the dual-, triple- and quadruple-SM properties of the polymer.

4. SMP Composites

4.1. Review of progress

The low stiffness and strength of SMPs is a limiting factor with respect to their industrial applicability. For this reason, significant attention was placed worldwide on dissimilar reinforcement strategies, leading to the development of various SMP composites. In early works, fillers such as chopped carbon, glass or Kevlar fibers were used to enhance the rubbery moduli of SMPs [190]. Woven fiberglass SMPU composites, for instance, displayed increased ultimate strength (by 50%) and improved Young's modulus (by almost 400%) towards their non-reinforced analogs [190]. Ohki *et al*. [191] demonstrated for SMPU (from Diaplex Co., Ltd., a subsidiary of MHI), which was used as matrix for chopped strand glass fibers, that an optimum fiber fraction between 10 and 20 wt% supports very low residual strains during thermo-mechanical cycling. They also reported that an increasing fraction of reinforcement leads to an increase in modulus and in recoverable force, whereas ductility and shape recoverability decrease. The latest progress in research on SMPU composites has been reviewed by Huang *et al*. [111].

In the following, some further elementary steps that could be made in the development of SMP composites are highlighted. Viry *et al*. [192] employed PVA as SMP matrix material for single walled carbon nanotubes (SWCNTs). The manufactured SMP composites revealed maximum recovery

stresses close to 150 MPa when deformed at temperatures that were in the vicinity of T_g = 80 °C of neat PVA, adjacently fixed through cooling under fixed strain and reheated. In a fascinating approach, the authors achieved an alignment of fillers through fiber drawing up to 500% of strain and removal of the polymer by thermal degradation. The remaining porous fibers were comprised of entangled CNTs, held together by van der Waals interactions, and had much better mechanical properties than random assemblies of nanotubes in bucky paper. Xu *et al*. [193] found that the incorporation of different nanofillers (alumina, silica and clay) into chemically cross-linked polystyrene gives different macroscopic properties, depending on the shape of the utilized nanofillers. As evidenced by both experimental and theoretical analysis, rod-shaped clay nanofillers have a stronger reinforcement influence than spherical nanoparticles such as Al_2O_3, due to their higher aspect ratio and ability to reinforce a polymer in multiple directions. Jung *et al*. [194] introduced nanostructured silica particles (Aerosil 200 from Degussa) into amorphous PU by sol-gel reactions. The used particles served as cross-links and reinforcing fillers. The most functionally reliable material, among the investigated PU-silica chemical hybrid formulations, contained 1 wt% of silica and revealed excellent shape fixities and recoverabilities of 99% up to the fourth thermo-mechanical cycle. In another example, Mondal and Hu [195] observed an improvement in shape recoverability from 85%, determined for non-reinforced SMPU, to 92% in the presence of 2.5 wt% multi-walled carbon nanotubes (MWCNTs). Koerner *et al*. [196] obtained uniform dispersions as proven by scanning electron microscopy (SEM) for 1 to 5 vol% of MWCNTs in Morthane ($T_{trans} = T_m$), which is a thermoplastic SMPU elastomer from Huntsman Polyurethanes. In comparison with neat Morthane, polymer carbon nanotube composites containing 2.9 vol% (5 wt%) MWCNTs exhibited improved shape fixity ratios (from 56 to 70% for ε_m = 250%) and increased recovery stresses from 0.6 MPa to 1.4 MPa, when passing the soft segmental melting transition. Deka *et al*. [197] studied Mesua ferrea L. seed oil-based, epoxy-modified hyperbranched PU composites with MWCNTs. The composites with 5, 10 and 20 wt% of epoxy resin revealed shape retentions between 74 and 87%, shape recoverabilities of 90 to 98% and significantly improved tensile strengths towards pristine hyperbranched PU. However, in some cases fillers are prone to have negative effects on the shape recoverability of an SMP due to their size and substantially higher stiffness compared to the matrix polymer. At high loading levels, they may even disturb the polymer networks responsible for SM functionality [198]. Razzaq and Frormann [199] have shown that loading an ether-based SMPU from Diaplex Co., Ltd. with 40 wt% AlN particles increases the thermal conductivity from 0.12 to 0.44 W/mK. SEM images revealed that the particles were well dispersed throughout the polymer matrix. The incorporation of 40 wt% AlN slightly increased the weak shape fixity ratio from about 43 to 45%, but lowered the shape recovery ratio by more than 20%. The composite's response times to heating were shortened upon increasing AlN filler contents. The lowering of transition temperature was confirmed by DSC; T_g fell from 51 to 45 °C. Park *et al*. [80] also investigated organic-inorganic hybrid PU. Using celite, a natural product composed of silica and alumina, in order to cross-link polymer chains gave materials with much better mechanical properties. Due to cross-linking effects at low celite content of 0.2 wt%, a strong increase in stress-at-break from 3.5 to 19 MPa could be observed. Increasing the celite content to 0.4 wt% even favored an increase in strain-at-break from originally about 880 to 2,470%. In terms of SM properties, the shape fixity ratio and shape recovery ratio improved with increasing celite content, both ratios of the first thermo-mechanical cycle were close to 100% for specimens containing 0.8 wt% celite. A different

approach was followed by Zhang *et al*. [200], who held inclusion complexes of *α*-cyclodextrin-poly(ethylene glycol) (PEG), which were incorporated into PEG, by solution casting. The *α*-cyclodextrin-PEG inclusion crystallites served as fixing phase and the PEG crystallites as reversible phase. The SM effect was examined by bending tests; recovery ratios of 97% were obtained for inclusion contents of 60 wt%.

Gall *et al*. [201] reported an increase in elastic modulus and micro-hardness by a factor of 3, when incorporating 40 wt% nanoparticulate SiC into a commercial thermoset epoxy-based SMP from Composite Technology Development, Inc. The observed phenomena were a direct consequence of the relatively high modulus/hardness of the employed reinforcements, which were well dispersed in the polymer matrix as proven by SEM. It could also be shown that the constrained bending recovery force in the nanocomposites increased by 50% with the addition of 20 wt% SiC. Ohki *et al*. [202] found an improvement in creep properties (rupture strain and time) and enhancement in resistance to cyclic loading for SMPU from Diaplex Co., Ltd., containing up to 30 wt% of chopped strand glass fibers of 3 mm length. Cao and Jana [203] reported on nanoclay PCL-based SMPU composites, for which good particle dispersion was evidenced by transmission electron microscopy (TEM). In this case, low filler contents of 1 wt% favored an increase in the magnitude of shape recovery stress by 20%. However, the presence of clay particles hindered soft segment crystallization and promoted phase mixing between hard and soft segments. Polymers with higher clay contents displayed more rapid relaxation processes of induced tensile stress, thus limiting the magnitude of shape recovery stress.

In an innovative approach, the electrical resistivity and electromagnetic interference (EMI) shielding effect (SE) of MWCNT/polyester-based SMPU composites was elucidated by Zhang *et al*. [204]. Apart from a clear tendency of decreasing electrical resistivity with increasing weight fraction of filler in the composites, the study gave stronger EMI SEs of the test materials with the increase in frequency from K band (8–26.5 GHz) over Q band (33–50 GHz) to V band (50–75 GHz). Under the same frequency condition, higher EMI SEs were detected for samples with larger thicknesses of up to 3 mm. At all frequency bands the EMI SEs increased with growing filler contents. For a material with 6.7 wt% filler at a thickness of 3 mm, the value of EMI SE exceeded over 30 dB for all three frequency bands; its maximum value even reached 65 dB. The employed MWCNTs were randomly distributed in the polymer matrix as evidenced by SEM.

4.2. Electrically conductive SMP composites

The demand to identify alternative strategies in order to heat SMPs above their transition temperature directed research to electrical sensitive SMPs filled with carbon nanotubes [34,35,37,205], carbon particles [30,36], conductive fibers [40], Ni powders [47,48], *etc*. Electrically induced actuation allows the convenient triggering of shape recovery by passing an electrical current through a composite [34,206]. For instance, loading PCL-based SMPU with 5 wt% of functionalized MWCNTs for interfacial bonding between polymer chains and nanotubes enabled Cho *et al*. [35] to completely recover the shape of their composite within 10 s through the application of a 40 V electrical potential. Another example for electric-field-triggered shape recovery was given by Leng *et al*. [207]. The application of 25 V to styrene-based SMP, filled with 5 wt% of carbon black and 2 wt% of short carbon fibers, resulted in shape recovery times of 50 s. In a closely related effort, the same group [208]

published another study on conducting styrene-based SMP composites. When filled with 10 vol% of homogenously distributed carbon nanopowder, samples revealed good shape recovery performances; within 90 s of Joule heating (30 V), the shape recoverability was estimated to be between 75 and 80%. Sahoo *et al*. [209] reported on the use of inherently conductive polypyrrole as coating layer for PCL-based SMPU, filled with MWCNTs. In shape recovery tests with bending mode, one specimen containing 20 wt% polypyrrole was able to recover within 25 s between 85 and 90% of its original shape at a constant electric potential of 40 V.

In a different approach, Lu *et al*. [210] investigated the lowering of electrical resistivity for the commercially available epoxy-based SMP resin Veriflex®E2 through blending carbon nanofibers with the resin and coating carbon nanopaper onto the surface of the composite. Due to the synergistic effects of fibers and paper, heat transfer was facilitated and the electrical resistivity of the SMP composite was 10^{16} times lower than for pure SMP resin. Nevertheless, the shortest detected shape recoveries took quite long (186 s) and shape recoverabilities were reduced with increasing carbon nanofiber contents, which was explained by the accumulation of interfacial friction effects between the SMP's macromolecular segments, carbon nanopaper and the blended carbon nanofiber particles.

Leng *et al*. [48] presented a convenient way to reduce the electrical resistivity of SMPU composites. The authors obtained electrically conductive composites by mixing 0.5 vol% Ni particles and 4–10 vol% carbon black with an SMPU ($T_{trans} = T_g$), which was dissolved in DMF. During volatilization of DMF, a low magnetic field was applied to the polymer/filler solution. As a result, conductive Ni powder chains formed and the electrical conductivity improved (Figure 2). This positive effect was based on the fact that the aligned Ni chains served as conductive channels to bridge small isolated carbon black aggregates.

Figure 2. Scanning electron microscopy (SEM) images of conductive SMPU containing 10 vol% of carbon black and 0.5 vol% of chained Ni. Inset: Zoom-in view of one Ni chain. Reprinted with permission from [48]. (© 2008, American Institute of Physics).

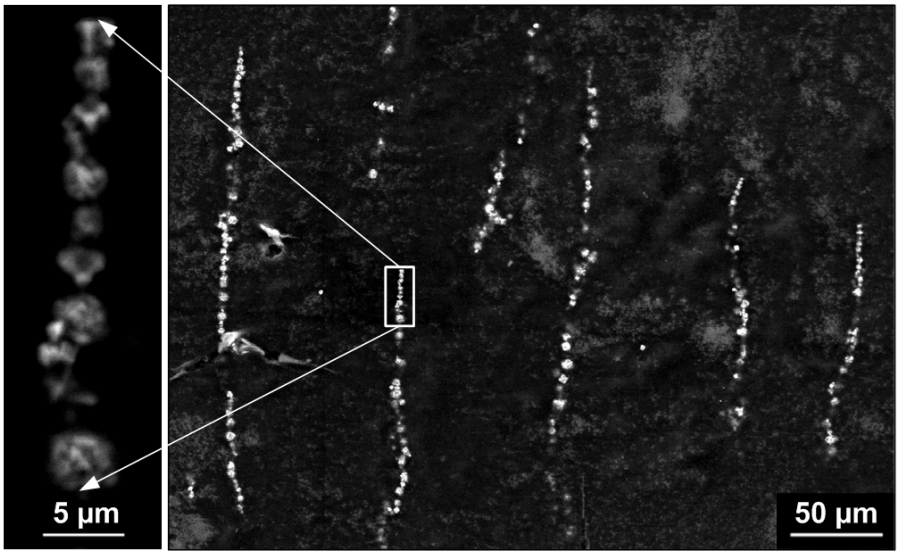

Although the uniform dispersion of fillers in polymer matrices is still challenging, the general concept allows imparting attractive material properties to SMPs. It is a widely held opinion in SMP research that indirect actuation methods may pave the way to new technology platforms.

4.3. Magnetosensitive SMP composites

Another indirect actuation method and alternative to direct heating (the increase of environmental temperature) is the inductive heating of magnetic particles, which are dispersed in an SMP. For this purpose an alternating magnetic field is applied, causing strong particle motion inside the polymer matrix and thus local heating effects. Some recent advances and fundamental insights in this field were given by Lendlein's group [211,212]. Since magnetically induced actuation allows the triggering of the SM effect in a remote and wireless manner, the technique should be applicable to medical devices.

The prerequisite for magneto-sensitivity in SMP composites is the uniform dispersion of suitable fillers inside the SMP matrix. Successful concepts turned out to be the integration of iron(III)oxide (Fe_2O_3 nanoparticles with a shell of SiO_2 to improve their dispersion within the SMP matrix) or mixed-valence iron(II,III)oxide (Fe_3O_4 nanoparticles) into thermoplastic SMPs [46], the incorporation of PCL-coated Fe_3O_4 particles within butyl acrylate networks cross-linked with oligo(ε-caprolactone) dimethacrylate (polymer shells may improve the dispensability of hybrid particles in suitable solvents [213]) [38], the filling of methacrylate-based thermoset SMP networks with Fe_3O_4 nanoparticles [214] and the integration of nickel zinc ferrite particles into ester-based SMPU from Diaplex Co., Ltd. [45]. Aside from polymer composites with classical dual-shape properties, the non-contact triggering of triple-shape effects in multiphase polymer nanocomposites was successfully made by Kumar *et al*. [215]. The authors embedded silica coated Fe_2O_3 nanoparticles in a (PCL/poly(cyclohexyl methacrylate) (PCHMA)) matrix, applied a one or two step shape programming procedure and unveiled triple-shape properties in an alternating magnetic field.

Despite the attractiveness of the non-contact SM triggering method, especially for medical applications such as surgical deployment, major challenges are still the increase in inductive heating efficiency [13,45] (the applied frequencies should not exceed the restrictive window of clinically usable frequencies (50–100 kHz) [216]), and in case of polymers with multi-shape capabilities the tailoring of transition temperatures in a region close to body temperature. If such attempts fail, the development of polymers, which allow combining different actuation methods, applicable in physiological environments, will be a convenient alternative.

5. Solvent Sensitive SMPs

Pioneering works in the area of solvent sensitive SMPs date back to 2004, when Huang's group [217] reported on the impact of moisture on SMPU specimens ($T_{trans} = T_g$) from MHI. The authors found that programmed specimens were not able to maintain their shape in humid air at 20 °C. The reason behind was the absorption of moisture, which strongly lowered the material's transition temperature (Figure 3). Since T_g fell below room temperature, shape recovery was initiated. The triggering of the SM effect was thus exclusively due to the plasticizer effect of the absorbed water molecules onto the polymer matrix. This shows that the lowering of transition temperature by diffusion

of low molecular weight molecules into polymer bulk is an interesting way to trigger a SM effect, while a polymer's temperature remains constant.

Figure 3. Changes in the SMPU's T_g and weight fraction (WF) of moisture *vs.* immersion time in water (20 °C). Reprinted with permission from [217] (© 2010, Institute of Physics Publishing).

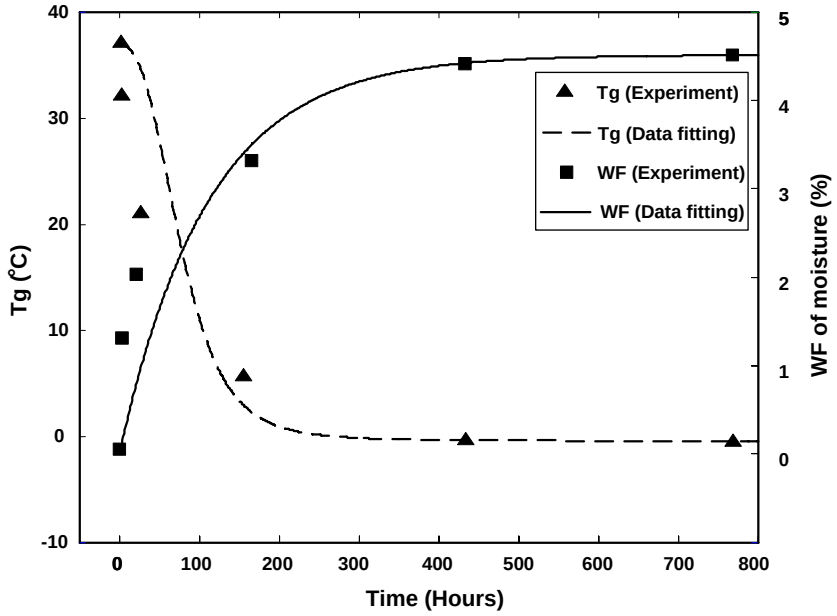

In two closely related publications, the same group extended their investigations to SMPU composites [36,218]. For composites containing carbon nanopowder as filler, much higher resistances towards humidity could be verified; higher contents of fillers even lowered moisture sensitivity. Among the two types of water species investigated, namely bound water (directly attached to the polymer backbone) and free water (clustered water), bound water was observed to strongly lower T_g, whereas the influence of free water on T_g seemed to be negligible. Chen *et al*. [53] contributed to widen the knowledge through investigating the moisture-sensitivity of SMPU containing pyridine moieties. Similar to the abovementioned works, the authors noted that the uptake of moisture lowered T_g and activated shape recovery on programmed specimens. The documented plasticizing effect of water was explained by the dissociation of hydrogen bonding between the involved pyridine ring and the N–H of the urethane entity. One of their samples was able to recover 95% of strain within 10 min at 32 °C and 80% relative humidity. Auxiliary studies from Du and Zhang [219] revealed that the transition temperature of PVA-based SMP ($T_{trans} = T_g$), chemically cross-linked with different contents of glutaraldehyde, was strongly affected by moisture. Due to the hydrophilic nature of PVA, water was taken up rapidly, so that T_g fell within half an hour from 61 to 29 °C and even decreased further to 25 °C within a total exposure time of 3 h. Following a completely different strategy, Jung *et al*. [220] realized for (PEG/1,4-phenylene diisocyanate (PDI)/POSS)-based SMPs the induction of moisture sensitivity through dissolution of the PEG soft segment constituent in water, resulting in specimen recovery from a programmed, ring-shaped geometry into an almost linear permanent shape within 5 min at 30 °C or, alternatively, within 10 s at 60 °C.

Although it is unlikely that other solvents than water are present in an SMP's environment, Lv *et al*. [52] have proven for commercially available styrene-based SM thermosetting resin that shape recovery can also be triggered through the uptake of DMF. The investigated material displayed a drop in T_g from 70 to 56 °C within 120 min of DMF immersion. Based on these works, Lu *et al*. [221] studied the effect of the solubility parameter on the recovery behavior of styrene-based SM thermosetting resin. The consideration of the results for specimen immersion in different solvents (ethyl acetate, ethyl formate and DMF) allowed verifying the relationship between the solvent solubility parameter and the rate of decrease in T_g. A clear tendency towards faster T_g decreases, tantamount to shorter recovery times, for solvents with higher solubility parameters was found. The results were in good agreement with the principle of solution theory of polymer physics [222].

In summary, the exploitation of SMP actuation through the diffusion of low molecular weight molecules into polymer bulk has just begun and could prove beneficial for various industries in the future; one important sector could be the medical industry.

6. Aging Effects in SMPs and Their Composites

Decisive criterions for the quality and reliability of SMPs and their composites [223] are the long-term mechanical and functional stability. The history of durability studies on SMPs goes back to 1988, when Shirai and Hayashi [54] reported for the first time on the physical (including SM) and chemical properties of a thermoplastic SMPU. Excellent heat resistance at 70 °C for 500 h and good weatherability even after 300 h of sunshine exposure, were proven by insignificant changes in the elastic modulus of the specimens. Good endurance to repeated loading was demonstrated by constant glass transition temperatures after cycling temperature between 5 and 40 °C, accompanied by regular stress-loading and unloading steps. The chemical resistance of the material was characterized in soaking tests; the material's volume changed within 5% in gasoline for 100 h at room temperature. Two years later, further results of soaking tests were reported by Hayashi [224]. The experiments revealed that the material's elongation capability virtually remained the same after the SMPU had been soaked for 24 h at 35 °C in an aqueous solution. At the same time, the tensile strength decreased by 27% and the glass transition temperature was reduced from 55 to 40 °C.

In line with aging processes in other materials, SM properties show aging in functionality and each SMP displays an individual aging behavior. Natural aging tests are representative, because they enable the reproduction of identical exposure conditions. Since such experiments are often time-consuming, accelerated aging tests, in which processes of deterioration are sped-up in the laboratory under fully controllable conditions, are used instead. Nevertheless, it is important to make sure, that no change in degradation mechanism takes place. Aging under drastic conditions allows elucidation of the chemical reactions involved (the degradation mechanism) and the physical consequences thereof in much shorter time frames. Recent investigations on the impact of hydrolysis (up to 68 d at 55 °C [225] and up to 8 d at 80 °C [225-227]) on poly(1,4-butylene adipate) (PBA)-based SMPU revealed a strong impairment of the thermo-mechanical properties. In dual-shape testing experiments, specimens were fixed through soft segment crystallization and shape recovery was triggered through soft segment melting. The testing results gave gradual increases in residual strain ε_p, associated with the amount of unrecoverable strain, and in transition temperature. The shape and total shape recoverabilities of the

polymer worsened as a consequence of degradation (Figure 4), which was accompanied by growth in soft segment crystallinity, as indicated by differential scanning calorimetry (DSC), and changes in phase separation.

In an effort to postpone the detected hydrolytic degradation effects, researchers from Bayer MaterialScience AG synthesized a hydrolysis-stabilized, PBA-based SMPU [228]. The concept turned out to be successful; the SMPU's long-term stability and thus long-term SM functionality improved as evidenced by a retard of the beginning of mechanical and functional impairment through hydrolysis (80 °C) by 44 d and 35 to 45 d, respectively. Hence, the SMPU revealed a 6.5-fold increase in durability towards embrittlement. Continuing cyclic thermo-mechanical measurements were carried out to elucidate the impairment of triple-shape properties of a PBA-based SMPU through hydrolysis (up to 8 d at 80 °C) [229].

In order to evaluate the key performance attributes of SMPs in application environments, Tandon *et al*. [230] characterized the durability of styrene-based and epoxy-based SMP resin materials (Veriflex^{TM} from Cornerstone Research Group, Inc.) after their exposure to different degradation scenarios, consisting of water conditioning at 25 and 49 °C (4 d), lube oil conditioning at room temperature and 49 °C (24 h) and UV conditioning (exposure to xenon arc at 63 °C for a different number of cycles, each cycle consisted of 102 min irradiation followed by 18 min light/water spray exposure). The good specimen resistance towards the different exposure scenarios was demonstrated by reasonable stress recovery data and excellent shape recoverabilities for styrene-based SMP (N = 1 and 2: close to 100%, including data for 75 UV cycles, but no lube oil data) and for epoxy-based SMP (N = 1:96–100%; N = 2:94–100%, including the data for 125 UV cycles and lube oil data). Styrene-based specimens displayed distinct sensitivity to lube oil as shown by the development of microcracks on their surface. In contrast, no microcracking was observed for epoxy-based SMP. Both types of SMPs developed a slight yellow tint in the course of UV exposure. Overall, epoxy-based SMP displayed superior mechanical properties and was identified as a likely candidate for morphing applications. Beyond this, continuing research needs were indicated for durability studies on fiber-reinforced SMP resins.

Further systematic studies were conducted by Meents *et al*. [231] from Cornerstone Research Group, Inc. The authors aimed at investigating the effect of both fresh and salt water (consisting of distilled water with 3.5 wt% NaCl, purity > 99.5%) on the healing performance of an epoxy-based SMP resin as integral part of a vehicle system, capable of autonomously monitoring its structural health. Upon damage identification the polymer was heated above its T_g through an integrated resistive heating element, which initiated the shape recovery process. The data, which exclusively derived from fracture toughness tests, suggested increased healing capability for a 14-day salt water soak *vs.* a 14-day fresh water soak. The authors speculated that the presence of water and non-water components of the saltwater, which could have remained in the polymer matrix, supported the healing process, hence promoting an increase in chain mobility. Nevertheless, it was expected that under healing conditions (132 °C) most water was driven off. The company intends to determine life cycle and system performance requirements for the implementation into operational marine vehicles in the future.

Figure 4. Effect of hydrolysis (80 °C) on the cyclic thermo-mechanical properties of PBA-based SMPU (maximum strain ε_m = 100%). **(a)** Changes are illustrated in ε–T test protocols, in which arrows are used to point out aging trends regarding T_{trans} and ε_p. **(b)** Evolution of shape fixity, shape recovery and total shape recovery ratios with cycling against immersion time. Reprinted with permission from [227] (© 2009, Elsevier).

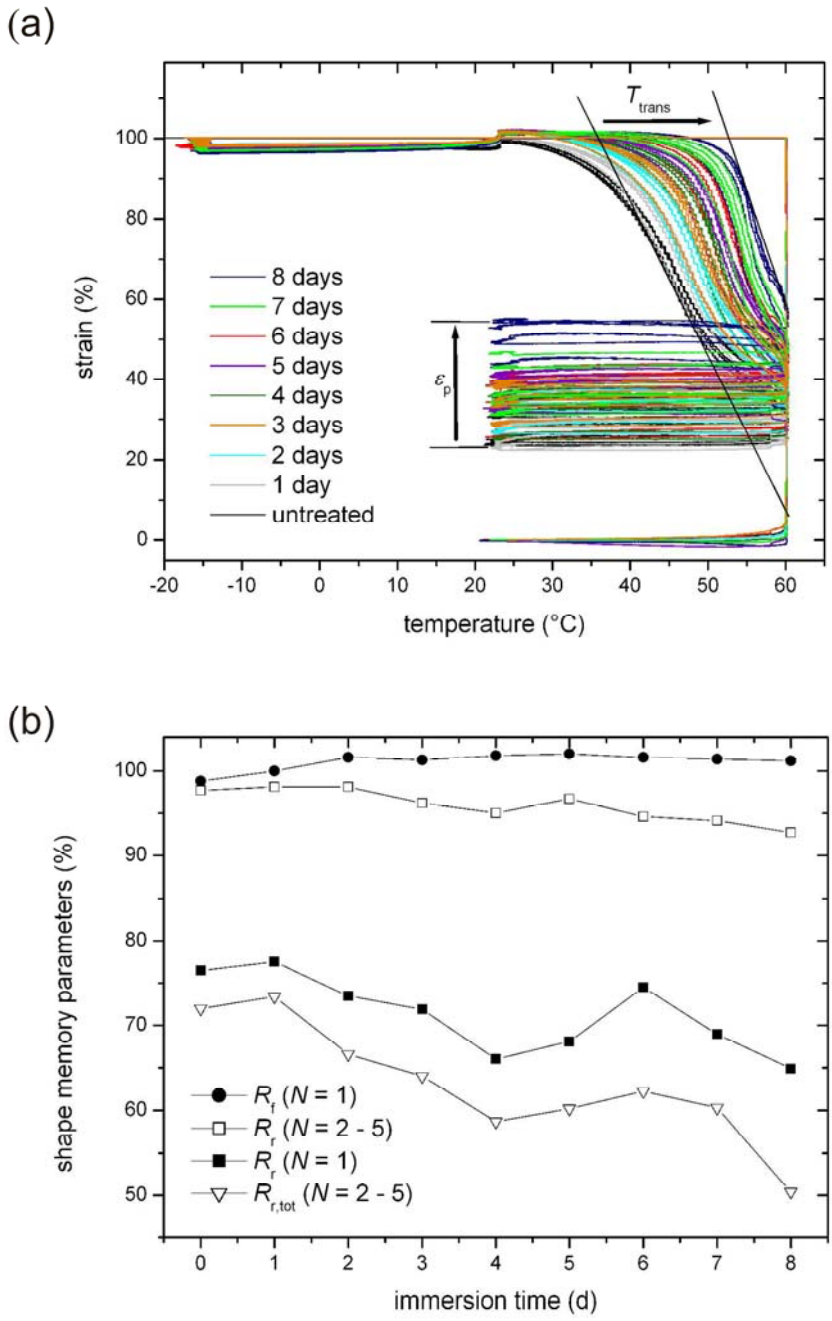

In the medical sector, only few functional supervision scenarios were reported so far. Zheng *et al*. [232] studied the effect of *in vitro* degradation on the SM properties of poly(D,L-lactide) (PDLLA)/*β*-tricalcium phosphate (*β*-TCP) composites with weight ratios of 1:1, 2:1 and 3:1. Specimens were immersed in phosphate buffer solution (PBS, pH = 7.4) at 37 °C and analyzed in regular time intervals. The shape recovery behavior of the specimens was determined from bending tests. In the course of degradation, the stress recovery ratios decreased within 56 d from about 98% to values in

between 56 and 67%. This effect may be associated with the cleavage of PDLLA chains and changes in the crystal phases of *β*-TCP. In another comprehensive study, Yu *et al*. [233] investigated the *in vitro* degradation behavior of SM nanocomposites consisting of cross-linked PCL and Fe_3O_4 nanoparticles. Due to degradation at 37 °C in PBS, their specimens revealed progressively weaker shape recoverabilities in static tensile tests with increasing filler fractions. For example, the shape recovery ratio of samples containing 15 wt% Fe_3O_4 decreased from 75% before degradation to 20% in the 12th week. At the same time, the shape recovery ratio dropped by about 35% for samples loaded with 5 wt% Fe_3O_4 and by about 25% for pristine material. It can be envisioned that a detailed investigation of enzymatic or hydrolytic degradation processes will become important in the medical field with the realization of innovative SMP concepts like removable implants or controllable drug release systems. In this connection it may be of interest to find out, in which time interval an SMP is able to reliably carry out predetermined shape changes inside a human body.

Another recent contribution was made by Zhang *et al*. [234]. The authors used Co-60 gamma rays to investigate the influence of irradiation on styrene-based SMP with $T_{trans} = T_g$. At a dose of 1×10^4 Gy, they witnessed a decrease in gel content from 35 to 30%, a reduction in tensile strength by −17% and a decrease in the DMA's tan δ peak associated with T_g from 87 to 82 °C. The shape recovery speed was identified as important functional characteristic and determined at different temperatures every 5 °C from 75 to 95 °C. In particular above and at 85 °C, the SMP's recovery speed was decelerated through irradiation, whereas at 75 and 80 °C it was the other way around. At 75 °C, for instance, irradiated SMP took 60 s to recover and pristine SMP 90 s. The discrepancy was explained by the fact that the polymer's T_g was lowered through irradiation, which increased the mobility of polymer chains at lower temperatures. Irradiation with Co-60 gamma rays is commonly used to sterilize medical equipment, but was not mentioned in this context by the authors. In order to be able to better assess the given results, it would be worth comparing them with the ones of those polymers, whose replacement is potentially considered.

Up to now, relatively little emphasis was placed on improving the thermal stability of SMPs. The thermal stability of polymers can be easily monitored by thermogravimetric analysis. Thermoplastic SMPUs undergo thermal degradation first via decomposition of urethane bonds before soft segments start to decompose [235,236]. The thermal stability of magnetite filled SMPU composites was investigated by Razzaq *et al*. [237]. The authors found that the fillers slightly increased the thermal stability towards the first decomposition step and explained the phenomenon by the higher thermal conductivity of the magnetite, which may favor better heat absorption, so that polyurethane chains start degrading at higher temperatures. Jana and Cho [238] investigated the thermal stability of PCL-based SMPU composites with different interfacial interactions, as obtainable through the proper choice of non-functionalized and functionalized MWCNTs. Higher thermal stabilities, e.g., higher activation energies at 10% degradation, were achieved for SMPUs with attached MWCNTs, which seemed to enable a better dispersion of the fillers in the polymer matrix. Looking for SMPs, which combine reasonable shape recoverabilities with good thermal stability, Jeon *et al*. [88] studied the SM properties of two different types of POSS hybrid copolymers, both containing 50 wt% POSS in a polynorbornene matrix ($T_{trans} = T_g$). Due to the presence of the fillers, T_g increased from 57 to 66 °C, when cyclopentyl (Cp) corner groups were chosen, and to 73 °C in case of cyclohexyl (Cy) corner groups. TEM measurements unveiled that the POSS macromers aggregated to form cylindrical domains. To

minimize stress relaxation and achieve good shape fixity, the studied films were quenched in liquid nitrogen after they were str*etc*hed in a water bath to ε_m = 300% at $T = T_g + 15$ °C. Although the presence of POSS molecules and their aggregates influenced the relaxation of polynorbornene chains, counteracting the recovery process and thus decreasing shape recoverabilities (from 92% for PN homopolymer to 84% for CpPN and 70% for CyPN, respectively), the advantage of such systems lies in their superior thermal stability.

7. Cycle Life of SMPs and Their Composites

The life cycle perspectives of an SMP can be estimated by running a large number of consecutive thermo-mechanical cycles, during which the durability of SM properties is followed. Interestingly, attention in literature was mainly directed to dual-shape polymers with "one-way" SM. Lin and Chen [174] reported on the cycle life of polyether-based SMPUs, which was examined by bending tests. One of their formulations revealed a small loss in shape recoverability by about 4% after running 200 SM cycles. Ohki *et al*. [191] investigated glass fiber reinforced SMPU composites and defined the "stress keeping ratio" as ratio of stress comparing the recovery stress in the *N*th cycle with that one of the first cycle. The measurement data for up to 60 consecutive cycles, generated from static tensile tests, revealed that the "stress keeping ratio" depends both on the weight fraction of the reinforcement and on the number of tested cycles. In the course of cycling, the loss in stress keeping ratio was strongest for bulk specimens and improved with increasing filler contents from 10 to 30 wt%. Xu *et al*. [79] reported the results of bending tests for Si–O–Si cross-linked organic/inorganic hybrid polyurethanes. They found that repeated cycling in air ($N > 50$) had no significant impact on the material's shape fixing abilities and shape recoverabilities, but cycling in water lowered the shape fixing abilities, which presumably is due to the plasticizer effect of water. Recent studies performed by Schmidt *et al*. [239] aimed at investigating the impairment of SM functionality through fatigue by studying commercially available SMP Veriflex™. After applying a series of $N = 19$ thermo-mechanical cycles (ε_m = 100%), the material displayed a steady decrease in shape recoverability and changed its surface from flat to wavy. In this connection, a surface wavelength of about 195 μm could be detected by optical microscopy (Figure 5).

In another approach, Schmidt *et al*. [240] also investigated the SM properties of a commercial, totally amorphous cycloaliphatic poly(ether urethane) (Tecoflex® from Lubrizol). The T_g of a mixed phase, which was used as switching phase, was 74 °C and the softening temperature of the hard domains was 120 °C as evidenced by DMA measurements. The results of 50-cycle thermo-mechanical measurements were dependent on the choice of the highest testing temperature. Higher maximum strains in the order 100, 200, 400 and 600% favored throughout lower shape recoverabilities at 90 °C; whereas at 80 °C a virtually opposite trend was indicated. In all cases, 15 °C was selected as low temperature.

To validate the cyclic repeatability and durability of PCL-based SMPU containing MWCNTs as conductive ingredients, Goo *et al*. [39] used a cyclic testing procedure, in which each cycle consisted of thermo-mechanical shape fixing, followed by triggering shape recovery through Joule heating. For this purpose, an electrical current of about 10 mA was applied. They found that specimen cycle life was dependent on the deformation conditions (maximum strain and temperature). For strains of 60%, a

maximum of 420 cycles could be run at 30 °C, higher strains of 100% allowed 150 cycles to be run, whereas 120 cycles could be run at 60% strain and 40 °C. The authors concluded that higher actuation temperatures induce property degradation as a result of the rapid movements of molecular chains.

Figure 5. Surface features of an SMP Veriflex^{TM} specimen as observed by optical microscopy. **(a)** Flat reflecting surface of pristine material with few scratches. **(b)** Wavy surface features after running 19 thermo-mechanical cycles. Reprinted with permission from [239]. (© 2008, Wiley-VCH Verlag GmbH & Co. KGaA).

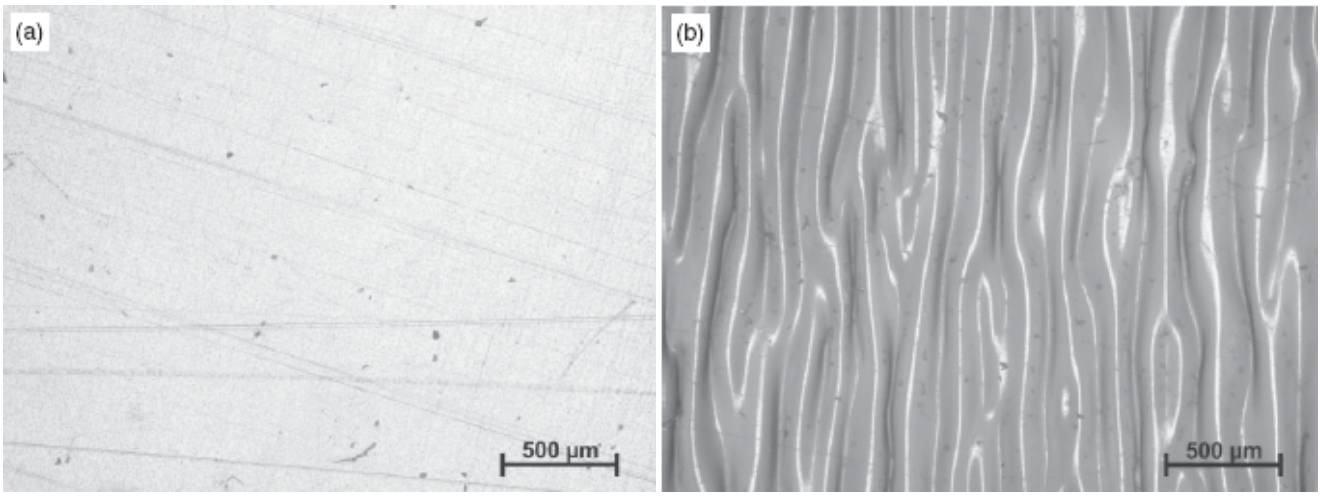

The given cycle life studies can be considered as a valuable basis for future characterizations of SMPs. For instance, reversible actuation is a vital factor in terms of the acceptance of SMPs in actuator applications, illustrating strong need for further research in this field.

8. SMPs Intended for Use in Medical Applications

One major research trend is the development of SMPs for medical applications. When considered as implant material, which e.g., can be inserted into a human body through a minimal invasive incision, application requirements for SMPs can be complex. SMPs must fulfill a series of characteristics such as biocompatibility and low cytotoxicity [149,241,242]. Beyond this, additional requirements can be hydrolytic degradability, specific SM functionality (e.g., a switching temperature close to body temperature) and homogeneous degradation properties [243]. Biodegradable SMPs with controllable degradation behavior provide interesting advantages over other implant materials, because much of today's follow-on surgery in removing the implants can thus be avoided. With this concept in mind, biodegradable SMPs based on poly(DL-lactide) and PCL [78,148, 244-249], blends based on poly(L-lactide-co-ε-caprolactone) and poly(L-lactide-co-glycolide) [250], SMPs based on bile acids [251,252] and many others [253-257] have been synthesized. Recent research trends regarding medical applications of SMPs have been summarized by Sokolowski *et al*. [149], Mather *et al*. [13], Small *et al*. [258] and Lendlein *et al*. [259]. To the envisioned technologies belong biodegradable sutures [148], drug carriers and delivery systems [212,260], tissue engineering scaffolds [261], dialysis needle adapters [262], annuloplasty rings [263], bone fillers [264], bone fracture fixation devices [265], micro-actuators to remove blood vessel clots [29], catheters and stents [71,246,266,267]

and self-deploying neuronal electrodes [268]. Recent progresses in miniaturization of SMP devices seem to point the way towards future surgery inside living cells [142,269]. As noted about three years ago by Dietsch and Tong [9], the majority of SMP patents lie in the medical sector. Major progress in this field is expected with the transfer of appropriate SMPs into clinical evaluation schemes.

9. SMP Foams

An example that illustrated the tremendous potential of SM technology is foams. The first patent on PU foam was issued in 1966 [270]. The altering of the relative foam density allows for an optimized trade-off between weight and mechanical properties. For this reason, SMP foaming is an important means to tailor material properties for application requirements [271,272]. The main advantage of this technology is that structures, when compressed and stored below a transition temperature, are a small fraction of their original size. Compressed SMP in open cellular (foam) structures can be used to erect structures that have various shapes and sizes, spanning from biomedical uses [241,273-275] like embolic sponges to morphing wings on advanced airframes [276]. Recognizing the importance of such self-deployable structures and their long-term storage capacities with respect to strain and stress, Huang and co-workers [277] investigated the material properties of compressed cold hibernated elastic memory (CHEM) polyurethane foam (T_{trans} = T_g) from MHI. The analysis of the effect of cold hibernation at 30 °C on CHEM foam revealed an expansion back to its original shape within approximately four days. The material behavior was attributed to the pretty high storage temperature of the foam, which was selected very close to the transition temperature. Using an appropriate SMPU with a higher T_g or the lowering of storage temperature were suggested by the authors to avoid or reduce the unwanted shape recovery effect. However, an adequate material performance could be achieved by applying a mechanical restraint during hibernation. In this case, complete shape recoverability could be detected even after a hibernation period of two months at 30 °C; beyond, the maximum recoverable stress was dependent on the amount of initially applied strain. Based on these observations, Tobushi *et al*. [179] studied the influence of shape holding conditions on the shape recoverability of an SMPU foam. The storage of unloaded, compressed specimens at a temperature well below the thermal transition (T_g—60 °C) revealed, that a programmed shape can even be kept for six months, independent of the applied maximum strain. Some fundamental studies focussing on the thermo-mechanical properties of epoxy-based SMP foam were recently published by Di Prima *et al*. [183,276,278].

10. Impact Testing to Study the Self-Healing Efficiency of SMPs

Polymers are susceptible to damage in the form of cracks, which lead to mechanical degradation. First concepts of self-healing materials were based on micro-capsules [279,280] or hollow glass fibers [281] with encased monomeric fluids, dispersed throughout a matrix material. During crack propagation, the dispersed capsules or fibers burst or fracture and release the fluid into the cracked region, where a catalyst initiates an *in situ* polymerization reaction, which finally patches a crack. SMP foams have been identified as useful alternative to the described single-use systems, since they are able to repeatedly heal matrix crackings, created e.g., by environmental effects. The reason behind is that an SMP is able to recover several times from its temporary, compression-programmed [181] into its permanent shape, thus repairing internal damages. In order to verify the huge potential of this

technology, extensive studies were published. In their recent discovery, Li and John [282] could show that SMP-based syntactic foam was able to heal impact damage repeatedly, efficiently and almost autonomously through a confined shape recovery process. The studied foam, which was composed of polystyrene-based SMP, glass microballoon and MWCNTs, was subjected to several impact-healing cycles. Each cycles consisted of heating above T_g = 62 °C, a 24 h application of constant compressive stress (0.05 MPa), two 3 h post-curing steps, slow cooling to room temperature and specimen unloading. After each shape fixing process the material was subjected to impact testing at room temperature and then healed through shape recovery. The excellent polymer performance was proven in seven impact-healing cycles through the ability to repeatedly heal the impact damages; microcracks could be reduced in length and microcrack openings were narrowed as a result of healing.

Nji *et al*. [150] reported on the impact tolerance and self-healing efficiency of a 3D woven fabric reinforced syntactic foam (SMP Veriflex^{TM}). For impact testing, a drop tower testing system equipped with a hammer of constant weight was used at two different velocities (3 and 3.5 m × s^{-1}), resulting in impact energies of 32 and 42 J, respectively. The performance of specimens, which were allowed to heal after impact with those which were not healed, revealed a decrease in healing efficiency with cycling and increasing impact load. At lower impact energies of 32 J at a peak impact load of 5.9 kN, the impact damages could be fully healed up to the fifth impact-healing cycle and specimens were perforated at the ninth impact for non-healed specimens, while healed specimens resisted until the 15th impact. Specimens impacted with 42 J of impact energy at a peak impact load of 6.1 kN, were perforated at the fifth impact, while healed specimens lasted until the seventh impact. The authors concluded that the different specimen behavior was due to an increase in unrecoverable damage as a consequence of growing microballoon crushing and fiber fracture with increasing impact energy. The given findings show that impact testing is a powerful tool to characterize the self-healing efficiency of SMP foams and indicate that the SMP technology is on the verge of entering applications, where self-healing plays a dominant role. Useful strategies may include outdoor concepts, in which long-term stability could be another important evaluation criterion.

11. Concluding Remarks

In this review, some of the main advances and findings in SMP research have been highlighted. SM technology is currently about to experience a revaluation due to the increase in functionality through advancements in synthesis and programming technology. The rising number of envisioned applications for SM materials renders SMP research an interesting field to study and emphasizes the need to introduce novel functional supervision scenarios. Some first promising steps have been made and reviewed. The steadily growing knowledge on SMPs is based on the extension of fundamental understanding of the decisive functional determinants, namely structure, morphology, processing and environment. Even though SMP research progresses rapidly, numerous challenges still remain in SMP development like the increase in recovery force, stiffness and strength, acceleration of recovery time, convenient triggering of SM effects, *etc*. Among the major challenges, the durability of SMPs is an important facet and should therefore deserve more attention in the future.

Acknowledgements

The author thanks Michael Maskos from BAM for fruitful discussions and acknowledges the Society of Plastics Engineers, the American Institute of Physics, the Institute of Physics Publishing, Elsevier and Wiley-VCH Verlag GmbH & Co. KGaA for giving permission to reprint one figure each.

References

1. Buehler, W.J.; Gilfrich, J.V.; Wiley, R.C. Effect of low-temperature phase changes on the mechanical properties of alloys near composition TiNi. *J. Appl. Phys.* **1963**, *34*, 1475-1477.
2. Tadaki, T.; Otsuka, K.; Shimizu, K. Shape memory alloys. *Annu. Rev. Mater. Sci.* **1988**, *18*, 25-45.
3. Otsuka, K.; Ren, X. Physical metallurgy of Ti–Ni-based shape memory alloys. *Prog. Mater. Sci.* **2005**, *50*, 511-678.
4. Schurch, K.E.; Ashbee, K.H.G. A near perfect shape-memory ceramic material. *Nature* **1977**, *266*, 706-707.
5. Swain, M.V. Shape memory behaviour in partially stabilized zirconia ceramics. *Nature* **1986**, *322*, 234-236.
6. Heuer, A.H.; Ruhle, M.; Marshall, D.B. On the thermoelastic martensitic transformation in tetragonal zirconia. *J. Am. Cer. Soc.* **1990**, *73*, 1084-1093.
7. Lendlein, A.; Kelch, S. Shape-memory polymers. *Angew. Chem. Int. Ed.* **2002**, *41*, 2034-2057.
8. Beloshenko, V.A.; Varyukhin, V.N.; Voznyak, Y.V. The shape memory effect in polymers. *Russ. Chem. Rev.* (*Engl. Transl.*) **2005**, *74*, 265-283.
9. Dietsch, B.; Tong, T. A review—features and benefits of shape memory polymers (SMPs). *J. Adv. Mater.* **2007**, *39*, 3-12.
10. Liu, C.; Qin, H.; Mather, P.T. Review of progress in shape-memory polymers. *J. Mater. Chem.* **2007**, *17*, 1543-1558.
11. Ratna, D.; Karger-Kocsis, J. Recent advances in shape memory polymers and composites: A review. *J. Mater. Sci.* **2008**, *43*, 254-269.
12. Rousseau, I.A. Challenges of shape memory polymers: A review of the progress toward overcoming SMP's limitations. *Polym. Eng. Sci.* **2008**, *48*, 2075-2089.
13. Mather, P.T.; Luo, X.; Rousseau, I.A. Shape memory polymer research. *Annu. Rev. Mater. Res.* **2009**, *39*, 445-471.
14. Leng, J.; Lu, H.; Liu, Y.; Huang, W.M.; Du, S. Shape-memory polymers—A class of novel smart materials. *MRS Bull.* **2009**, *34*, 848-855.
15. Hirai, T.; Maruyama, H.; Suzuki, T.; Hayashi, S. Shape memorizing properties of a hydrogel of poly(vinyl alcohol). *J. Appl. Polym. Sci.* **1992**, *45*, 1849-1855.
16. Hirai, T.; Maruyama, H.; Suzuki, T.; Hayashi, S. Effect of chemical cross-linking under elongation on shape restoring of poly(vinyl alcohol) hydrogel. *J. Appl. Polym. Sci.* **1992**, *46*, 1449-1451.
17. Osada, Y.; Matsuda, A. Shape memory in hydrogels. *Nature* **1995**, *376*, 219.

18. Mano, J.F. Stimuli-responsive polymeric systems for biomedical applications. *Adv. Eng. Mater.* **2008**, *10*, 515-527.
19. Ahn, S.-K.; Kasi, R.M.; Kim, S.C.; Sharma, N.; Zhou, Y. Stimuli-responsive polymer gels. *Soft. Matter.* **2008**, *4*, 1151-1157.
20. Voit, W.; Ware, T.; Dasari, R.R.; Smith, P.; Danz, L.; Simon, D.; Barlow, S.; Marder, S.R.; Gall, K. High-strain shape-memory polymers. *Adv. Funct. Mater.* **2010**, *20*, 162-171.
21. van Humbeeck, J. Shape memory alloys: A material and a technology. *Adv. Eng. Mater.* **2001**, *3*, 837-850.
22. Feninat, F.E.; Laroche, G.; Fiset, M.; Mantovani, D. Shape memory materials for biomedical applications. *Adv. Eng. Mater.* **2002**, *4*, 91-104.
23. Hornbogen, E. Comparison of shape memory metals and polymers. *Adv. Eng. Mater.* **2006**, *8*, 101-106.
24. Hu, J.; Yang, Z.; Yeung, L.; Ji, F.; Liu, Y. Crosslinked polyurethanes with shape memory properties. *Polym . Int.* **2005**, *54*, 854-859.
25. Hu, J.L.; Ji, F.L.; Wong, Y.W. Dependency of the shape memory properties of a polyurethane upon thermomechanical cyclic conditions. *Polym. Int.* **2005**, *54*, 600-605.
26. Díaz Lantada, A.; Lafont Morgado, P.; Mũoz Sanz, J.L.; Mũoz García, J.; Munoz-Guijosa, J.M.; Echvarri Otero, J. Intelligent structures based on the improved activation of shape memory polymers using Peltier cells. *Smart. Mater. Struct.* **2010**, doi: 10.1088/0964-1726/19/5/055022.
27. Jiang, H.; Kelch, S.; Lendlein, A. Polymers move in response to light. *Adv. Mater.* **2006**, *18*, 1471-1475.
28. Lendlein, A.; Jiang, H.; Jünger, O.; Langer, R. Light-induced shape-memory polymers. *Nature* **2005**, *434*, 879-882.
29. Maitland, D.J.; Metzger, M.F.; Schumann, D.; Lee, A.; Wilson, T.S. Photothermal properties of shape memory polymer micro-actuators for treating stroke. *Lasers Surg. Med.* **2002**, *30*, 1-11.
30. Koerner, H.; Price, G.; Pearce, N.A.; Alexander, M.; Vaia, R.A. Remotely actuated polymer nanocomposites—stress-recovery of carbon-nanotube-filled thermoplastic elastomers. *Nature Mater.* **2004**, *3*, 115-120.
31. Zhang, D.; Liu, Y.; Leng, J. Infrared laser-activated shape memory polymer. *Proc. SPIE Int. Soc. Opt. Eng*. **2008**, doi:10.1117/12.776109.
32. Leng, J.; Wu, X.; Liu, Y. Infrared light-active shape memory polymer filled with nanocarbon particles. *J. Appl. Polym. Sci.* **2009**, *114*, 2455-2460.
33. Leng, J.; Zhang, D.; Liu, Y.; Yu, K.; Lan, X. Study on the activation of styrene-based shape memory polymer by medium-infrared laser light .*Appl. Phys. Lett.* **2010**, doi: 10.1063/1.3353970.
34. Goo, N.S.; Paik, I.H.; Yoon, K.J.; Jung, Y.C.; Cho, J.W. Actuation of MAV control surface using conducting shape memory polymer actuator. *Proc. SPIE Int. Soc. Opt. Eng*. **2004**, *5390*, 194-201.
35. Cho, J.W.; Kim, J.W.; Jung, Y.C.; Goo, N.S. Electroactive shape-memory polyurethane composites incorporating carbon nanotubes. *Macromol. Rapid Commun.* **2005**, *26*, 412-416.
36. Yang, B.; Huang, W.M.; Li, C.; Li, L.; Chor, J.H. Qualitative separation of the effects of carbon nano-powder and moisture on the glass transition temperature of polyurethane shape memory polymer. *Scr. Mater.* **2005**, *53*, 105-107.

37. Paik, I.H.; Goo, N.S.; Jung, Y.C.; Cho, J.W. Development and application of conducting shape memory polyurethane actuators. *Smart. Mater. Struct.* **2006**, *15*, 1476-1482.
38. Schmidt, A.M. Electromagnetic activation of shape memory polymer networks containing magnetic nanoparticles. *Macromol. Rapid Commun*. **2006**, *27*, 1168-1172.
39. Goo, N.S.; Paik, I.H.; Yoon, K.J. The durability of a conducting shape memory polyurethane actuator. *Smart. Mater. Struct*. **2007**, *16*, N23-N26.
40. Leng, J.S.; Lv, H.B.; Liu, Y.J.; Du, S.Y. Electroactive shape-memory polymer filled with nanocarbon particles and short carbon fibers. *Appl. Phys. Lett.* **2007**, doi: 10.1063/1.2790497.
41. Meng, Q.; Hu, J.; Yeung, L. An electro-active shape memory fibre by incorporating multi-walled carbon nanotubes. *Smart Mater. Struct.* **2007**, *16*, 830-836.
42. Lv, H.B.; Leng, J.S.; Du, S.Y. Electro-induced shape-memory polymer nanocomposite containing conductive particles and short fibers. *Proc. SPIE Int. Soc. Opt. Eng*. **2008**, *6929*, doi:10.1117/12.775736.
43. Meng, Q.; Hu, J. A review of shape memory polymer composites and blends. *Composites A* **2009**, *40*, 1661-1672.
44. Liu, Y.; Lv, H.; Lan, X.; Leng, J.S.; Du, S. Review of electro-active shape-memory polymer composite. *Compos. Sci. Technol.* **2009**, *69*, 2064-2068.
45. Buckley, P.R.; Mckinley, G.H.; Wilson, T.S.; Small, W.; Benett, W.J.; Bearinger, J.P.; Mcelfresh, M.W.; Maitland, D.J. Inductively heated shape memory polymer for the magnetic actuation of medical devices. *IEEE Trans. Biomed. Eng.* **2006**, *53*, 2075-2083.
46. Mohr, R.; Kraftz, K.; Weigel, T.; Lucka-Gabor, M.; Moneke, M.; Lendlein, A. Initiation of shape-memory effect by inductive heating of magnetic nanoparticles in thermoplastic polymers. *Proc. Nat. Acad. Sci. USA* **2006**, *103*, 3540-3545.
47. Leng, J.S.; Lan, X.; Liu, Y.J.; Du, S.Y.; Huang, W.M.; Liu, N.; Phee, S.J.; Yuan, Q. Electrical conductivity of thermoresponsive shape-memory polymer with embedded micron sized Ni powder chains. *Appl. Phys. Lett.* **2008**, doi: 10.1063/1.2829388.
48. Leng, J.S.; Huang, W.M.; Lan, X.; Liu, Y.J.; Du, S.Y. Significantly reducing electrical resistivity by forming conductive Ni chains in a polyurethane shape-memory polymer/carbon-black composite. A*ppl. Phys. Lett.* **2008**, doi: 10.1063/1.2931049.
49. Woojin, L. Polymer Gel Based Actuator: Dynamic Model of Gel for Real Time Control. Ph.D. Thesis, Massachusetts Institute of Technology, Cambridge, MA, USA, 1996.
50. Huang, W.M.; Yang, B.; An, L.; Li, C.; Chan, Y.S. Water-driven programmable polyurethane shape memory polymer: Demonstration and mechanism. *Appl. Phys. Lett.* **2005**, doi: 10.1063/1.1880448.
51. Yang, B.; Huang, W.M.; Li, C.; Li, L. Effects of moisture on the thermomechanical properties of a polyurethane shape memory polymer. *Polymer* **2006**, *47*, 1348-1356.
52. Lv, H.; Leong, J.; Liu, Y.; Du, S. Shape-memory polymer in resonse to solution. *Adv. Eng. Mater*. **2008**, *10*, 592-595.
53. Chen, S.; Hu, J.; Yuen, C.-W.; Chan, L. Novel moisture-sensitive shape memory polyurethanes containing pyridine moieties. *Polymer* **2009**, *50*, 4424-4428.
54. Shirai, Y.; Hayashi, S.-I. *Development of Polymeric Shape Memory Material*; Mitsubishi Heavy Industries, Inc.: Nagoya, Japan, 1988.

55. Bellin, I.; Kelch, S.; Langer, R.; Lendlein, A. Polymeric triple-shape materials. *Proc. Nat. Acad. Sci. USA* **2006**, *103*, 18043-18047.
56. Pretsch, T. Triple-shape properties of a thermoresponsive poly(ester urethane). *Smart Mater. Struct.* **2010**, doi: 10.1088/0964-1726/19/1/015006.
57. Xie, T. Tunable polymer multi-shape memory effect. *Nature* **2010**, *464*, 267-270.
58. Chung, T.; Romo-Uribe, A.; Mather, P.T. Two-way reversible shape memory in a semicrystalline network. *Macromolecules* **2008**, *41*, 184-192.
59. Qin, H.; Mather, P.T. Combined one-way and two-way shape memory in a glass-forming nematic network. *Macromolecules* **2009**, *42*, 273-280.
60. de Blonk, B.J.; Lagoudas, D.C. Actuation of elastomeric rods with embedded two-way shape memory alloy actuators. *Smart Mater. Struct.* **1998**, *7*, 771-783.
61. Wei, Z.G.; Sandström, R.; Miyazaki, S. Shape-memory materials and hybrid composites for smart systems. *J. Mater. Sci.* **1998**, *33*, 3743-3762.
62. Sperling, L.H. *Introduction to Physical Polymer Science*; John Wiley & Sons: New York, NY, USA, 2006.
63. Yakacki, C.M.; Shandas, R.; Lanning, C.; Rech, B.; Eckstein, A.; Gall, K. Unconstrained recovery characterization of shape-memory polymer networks for cardiovascular applications. *Biomaterials* **2007**, *28*, 2255-2263.
64. Safranski, D.L.; Gall, K. Effect of chemical structure and crosslinking density on the thermo-mechanical properties and toughness of (meth)acrylate shape memory polymer networks. *Polymer* **2008**, *49*, 4446-4455.
65. James, H.M.; Guth, E. Theory of the elastic properties of rubber. *J. Chem. Phys.* **1943**, *11*, 455-481.
66. Chen, W.P.; Kenney, D.J. Study of phase separation in polyurethane using paramagnetic labels. effect of soft segment molecular weight, structure, and thermal history. *J. Polym. Sci. B Polym. Phys.* **1991**, *29*, 1513-1524.
67. Heintz, A.M.; Duffy, D.J.; Hsu, S.L.; Suen, W.; Chu, W.; Paul, C.W. Effects of reaction temperature on the formation of polyurethane prepolymer structures. *Macromolecules* **2003**, *36*, 2695-2704.
68. Pereira, I.M.; Oréfice, R.L. The morphology and phase mixing studies on poly(ester–urethane) during shape memory cycle. *J. Mater. Sci.* **2010**, *45*, 511-522.
69. Kagami, Y.; Gong, J.P.; Osada, Y. Shape memory behaviors of crosslinked copolymers containing stearyl acrylate. *Macromol. Rapid Commun.* **1996**, *17*, 539-543.
70. Flory, P.J. *Principles of Polymer Chemistry*; Cornell University Press Ithaca: New York, NY, USA, 1953.
71. Gall, K.; Yakacki, C.M.; Liu, Y.P.; Shandas, R.; Willett, N.; Anseth, K.S. Thermomechanics of the shape memory effect in polymers for biomedical applications. *J. Biomed. Mater. Res.* **2005**, *73A*, 339-348.
72. Takahashi, T.; Hayashi, N.; Hayashi, S. Structure and properties of shape-memory polyurethane block copolymers. *J. Appl. Polym. Sci*.**1996**, *60*, 1061-1069.
73. Kim, B.K.; Lee, S.Y.; Xu, M. Polyurethanes having shape memory effects. *Polymer* **1996**, *37*, 5781-5793.

74. Li, F.; Zhang, X.; Hou, J.; Xu, M.; Luo, X.; Ma, D.; Kim, B.K. Studies on thermally stimulated shape memory effect of segmented polyurethanes. *J. Appl. Polym. Sci.* **1997**, *64*, 1511-1516.
75. Lin, J.R.; Chen, L.W. Shape-memorized crosslinked ester-type polyurethane and its mechanical viscoelastic model. *J. Appl. Polym. Sci.* **1999**, *73*, 1305-1319.
76. Jeong, H.M.; Lee, J.B.; Lee, S.Y.; Kim, B.K. Shape memory polyurethane containing mesogenic moiety. *J. Mater. Sci.* **2000**, *35*, 279-283.
77. Jeong, H.M.; Lee, S.Y.; Kim, B.K. Shape memory polyurethane containing amorphous reversible phase. *J. Mater. Sci.* **2000**, *35*, 1579-1583.
78. Wang, W.; Ping, P.; Chen, X.; Jing, X. Polylactide-based polyurethane and its shape-memory behavior. *Eur. Polym. J.* **2006**, *42*, 1240-1249.
79. Xu, J.; Shi, W.; Pang, W. Synthesis and shape memory effects of Si–O–Si cross-linked hybrid polyurethanes. *Polymer* **2006**, *47*, 457-465.
80. Park, J.S.; Chung, Y.-C.; Lee, S.D.; Cho, J.W.; Chun, B.C. Shape memory effects of polyurethane block copolymers cross-linked by celite. *Fiber. Polym.* **2008**, *9*, 661-666.
81. Chung, Y.C.; Choi, J.H.; Chun, B.C. Shape-memory effects of polyurethane copolymer cross-linked by dextrin. *J. Mater. Sci.* **2008**, *43*, 6366-6373.
82. Sun, X.; Ni, X. Block Copolymer of trans-polyisoprene and urethane segment: Crystallization behavior and morphology. *J. Appl. Polym. Sci.* **2004**, *94*, 2286-2294.
83. Ni, X.; Sun, X. Block copolymer of trans-polyisoprene and urethane segment: Shape memory effects. *J. Appl. Polym. Sci.* **2006**, *100*, 879-885.
84. Wang, M.; Luo, X.; Zhang, X.; Ma, D. Shape memory properties in poly(ethylene oxide)-poly(ethylene terephthalate) copolymers. *Polym. Adv. Technol.* **1997**, *8*, 136-139.
85. Luo, X.; Zhang, X.; Wang, M.; Ma, D.; Xu, M.; Li, F. Thermally stimulated shape-memory behavior of ethylene oxide-ethylene terephthalate segmented copolymer. *J. Appl. Polym. Sci.* **1997**, *64*, 2433-2440.
86. Wang, M.; Zhang, L. Recovery as a measure of oriented crystalline structure in poly(ether ester)s based on poly(ethylene oxide) and poly(ethylene terephthalate) used as shape memory polymers. *J. Polym. Sci. B Polym. Phys.* **1999**, *37*, 101-112.
87. Mather, P.T.; Jeon, H.; Romo-Uribe, A.; Haddad, T.S.; Lichtenhan, J.D. Mechanical Relaxation and Microstructure of Poly(norbornyl-POSS) Copolymers. *Macromolecules* **1999**, *32*, 1194-1203.
88. Jeon, H.G.; Mather, P.T.; Haddad, T.S. Shape memory and nanostructure in poly(norbornyl-POSS) copolymers. *Polym. Int.* **2000**, *49*, 453-457.
89. Jeong, H.M.; Song, J.H.; Chi, K.W.; Kim, I.; Kim, K.T. Shape memory effect of poly(methylene-1,3-cyclopentane) and its copolymer with polyethylene. *Polym. Int.* **2002**, *51*, 275-280.
90. Nakayama, K. Properties and applications of shape-memory polymers. *Int. Polym. Sci. Tech.* **1991**, *18*, T43-48.
91. Kasprzak, S.E.; Martin, B.; Raj, T.; Gall, K. Synthesis and thermomechanical behavior of (qua)ternary thiol-ene(/acrylate) copolymers. *Polymer* **2009**, *50*, 5549-5558.
92. Lendlein, A.; Schmidt, A.M.; Langer, R. AB-polymer networks based on oligo(e-caprolactone) segments showing shape-memory properties. *Proc. Nat. Acad. Sci. USA* **2001**, *98*, 842-847.

93. Lendlein, A.; Schmidt, A.M.; Schroeter, M.; Langer, R. Shape-Memory polymer networks from oligo(ε-caprolactone)dimethacrylates. *J. Polym. Sci. A Polym. Chem.* **2005**, *43*, 1369-1381.
94. Warren, P.D.; McGrath, D.V.; Vande Geest, J.P. Effect of crosslinker length and composition on the hydrophobicity and thermomechanical response of acrylate-based shape-memory polymers. *Macromol. Mater. Eng.* **2010**, *295*, 386-396.
95. Yang, F.; Zang, S.; Li, J.C.M. Impression recovery of amorphous polymers. *J. Elect. Mater.* **1997**, *26*, 859-862.
96. Safranski, D.L.; Gall, K. Effect of chemical structure and crosslinking density on the thermo-mechanical properties and toughness of (meth)acrylate shape memory polymer networks. *Polymer* **2008**, *49*, 4446-4455.
97. Naga, N.; Tsuchiya, G.; Toyota, A. Synthesis and properties of polyethylene and polypropylene containing hydroxylated cyclic units in the main chain. *Polymer* **2006**, *47*, 520-526.
98. Beloshenko, V.A.; Beigelzimer, Y.E.; Borzenko, A.P.; Varyukhin, V.N. Shape-memory effect in polymer composites with a compactible filler. *Mech. Comp. Mater.* 2003, *39*, 255-264.
99. Liu, Y.; Gall, K.; Dunn, M.L.; McCluskey, P. Thermomechanics of shape memory polymer nanocomposites. *Mech. Mat.* **2004**, *36*, 929-940.
100. Gall, K.; Dunn, M.L.; Liu, Y.; Stefanic, G.; Balzar, D. Internal stress storage in shape memory polymer nanocomposites. *Appl. Phys. Lett.* **2004**, *85*, 290-292.
101. Liu, Y.; Gall, K.; Dunn, M.L.; Greenberg, A.R.; Diani, J. Thermomechanics of shape memory polymers: Uniaxial experiments and constitutive modeling. *Int. J. Plast.***2006**, *22*, 279-313.
102. Jeong, H.M.; Ahn, B.K.; Kim, B.K. Miscibility and shape memory effect of thermoplastic polyurethane blends with phenoxy resin. *Eur. Polym. J.* **2001**, *37*, 2245-2252.
103. Jeong, H.M.; Song, J.H.; Lee, S.Y.; Kim, B.K. Miscibility and shape memory property of poly(vinyl chloride)/thermoplastic polyurethane blends. *J. Mater. Sci.* **2001**, *36*, 5457-5463.
104. Kolesov, I.S.; Radusch, H.-J. Multiple shape-memory behavior and thermal-mechanical properties of peroxide cross-linked blends of linear and short-chain branched polyethylenes. *eXPRESS Polym. Lett.* **2008**, *2*, 461-473.
105. Zhu, G.; Xu, S.; Wang, J.; Zhang, L. Shape memory behaviour of radiation-crosslinked PCL/PMVS blends. *Radiat. Phys. Chem.* **2006**, *75*, 443-448.
106. Weiss, R.A.; Izzo, E.; Mandelbaum, S. New design of shape memory polymers: Mixtures of an elastomeric ionomer and low molar mass fatty acids and their salts. *Macromolecules* **2008**, *41*, 2978-2980.
107. Zhang, H.; Wang, H.; Zhong, W.; Du, Q. A novel type of shape memory polymer blend and the shape memory mechanism. *Polymer* **2009**, *50*, 1596-1601.
108. Radusch, H.-J.; Kolesov, I. Shape-memory behavior of peroxidic cross-linked polyethylene based blends. *Chem. Listy* **2009**, *103*, S33-S35.
109. Behl, M.; Ridder, U.; Feng, Y.; Kelch, S.; Lendlein, A. Shape-memory capability of binary multiblock copolymer blends with hard and switching domains provided by different components. *Soft Matter* **2009**, *5*, 676-684.
110. Zhang, S.; Feng, Y.; Zhang, L.; Sun, J.; Xu, X.; Xu, Y. Novel Interpenetrating Networks with Shape-Memory Properties. *J. Polym. Sci. A Polym. Chem.* **2007**, *45*, 768-775.

111. Huang, W.M.; Yang, B.; Zhao, Y.; Ding, Z. Thermo-moisture responsive polyurethane shape-memory polymer and composites: a review. *J. Mater. Chem.* **2010**, *20*, 3367-3381.
112. Keihl, M.M.; Bortolin, R.S.; Sanders, B.; Joshi, S.; Tidwell, Z. Mechanical properties of shape memory polymers for morphing aircraft applications. *Proc. SPIE* **2005**, *5762*, 143-151.
113. Thill, C.; Etches, J.; Bond, I.; Potter, K.; Weaver, P. Morphing skins. *Auronaut J.* **2008**, *112*, 117-139.
114. Yu, K.; Sun, S.; Liu, L.; Zhang, Z.; Liu, Y.; Leng, J. Novel deployable morphing wing based on SMP composite. *Proc. SPIE* **2009**, doi: 10.1117/12.845408.
115. Yu, K.; Yin, W.; Liu, Y.; Leng, J. Application of SMP composite in designing a morphing wing. *Proc. SPIE* **2009**, doi: 10.1117/12.839363.
116. Yu, K.; Yin, W.; Sun, S.; Liu, Y.; Leng, J. Design and analysis of morphing wing based on smp composite. *Proc. SPIE* **2009**, doi: 10.1117/12.815712.
117. Sofla, A.Y.N.; Meguid, S.A.; Tan, K.T.; Yeo, W.K. Shape morphing of aircraft wing: Status and challenges. *Mater. Des.* **2010**, *31*, 1284-1292.
118. Enomoto, M.; Suehiro, K.; Muraoka, Y.; Inoue, K.; Sumita, M. Physical properties of polyurethane blend dope-coated fabrics. *Text. Res. J.* **1997**, *67*, 601-608.
119. Russel, D.A.; Hayashi, S. Potential uses of shape memory film in clothing. *Tech. Text. Int.* **1999**, *8*, 17-19.
120. Mattila, H.R. *Intelligent Textiles and Clothing*; Woodhead Publishing Limited and CRC Press LLC: Cambridge, UK, 2006.
121. Meng, Q.; Hu, J.; Zhu, Y.; Lu, J.; Liu, Y. Morphology, phase separation, thermal and mechanical property differences of shape memory fibres prepared by different spinning methods. *Smart Mater. Struct.* **2007**, *16*, 1192-1197.
122. Hu, J. *Shape Memory Polymers and Textiles*; Woodhead Publishing Limited and CRC Press LLC: Cambridge, UK, 2007.
123. Hu, J.; Meng, H.; Zhu, Y.; Liu, Y.; Lv, J.; Ji, F.; Liu, B.; Yeung, L.; Shen, L.; Hu, Y.; Han, J.; Li, W.; Kennedy, J.F.; Onkaraiah, P.; Liu, Y.; Zeng, W.; Luo, H.; Chen, S.; Li, Y.; Zhuo, H.; Zheng, Y.; Zhang, C. An overview of stimuli-responsive polymers for smart textile applications. *Carb. Polym.* **2010**, doi:10.1016/j.carbpol.2010.1002.1044.
124. Xie, T.; Xiao, X. Self-peeling reversible dry adhesive system. *Chem. Mater.* **2008**, *20*, 2866-2868.
125. Kim, S.; Sitti, M.; Xie, T.; Xiao, X. Reversible dry micro-fibrillar adhesives with thermally controllable adhesion. *Soft Matter* **2009**, *5*, 3689-3693.
126. Mondal, S.; Hu, J.L.; Yong, Z. Free volume and water vapor permeability of dense segmented polyurethane membrane. *J. Membr. Sci.* **2006**, *280*, 427-432.
127. Meng, Q.; Hu, J.; Mondal, S. Thermal sensitive shape recovery and mass transfer properties of polyurethane/modified MWNT composite membranes synthesized via *in situ* solution pre-polymerization. *J. Membr. Sci.* **2008**, *319*, 102-110.
128. Everhart, M.C.; Stahl, J. Reusable shape memory polymer mandrels. *Proc. SPIE* **2005**, *5762*, 27-34.
129. Everhart, M.C.; Stahl, J. High strain fiber reinforced reusable shape memory polymer mandrels. *Int. SAMPE Symp. Exhib.* **2005**, *50*, 955-965.

130. Everhart, M.C.; Nickerson, D.M.; Hreha, R.D. High-temperature reusable shape memory polymer mandrels. *Proc. SPIE* **2006**, doi:10.1117/12.659950.
131. Gall, K.; Mikulas, M.; Munshi, N.A.; Tupper, M. Carbon fiber reinforced shape memory polymer composites. *J. Intell. Mater. Sys. Struct.* **2000**, *11*, 877-886.
132. Lake, M.S.; Campbell, D. The fundamentals of designing deployable structures with elastic memory composites. *IEEE Trans. Aerosp. Conf. Proc.* **2004**, *4*, 2745-2756.
133. Campbell, D.; Maji, A.; Asce, F. Failure mechanisms and deployment accuracy of elastic-memory composites. *J. Aerosp. Eng.* **2006**, *3*, 184-193.
134. Sokolowski, W.; Tan, S.; Willis, P.; Pryor, M. Shape memory self-deployable structures for solar sails. *Proc. SPIE* **2008**, doi:10.1117/12.814301.
135. Liu, Y.; Han, C.; Tan, H.; Du, X. Thermal, mechanical and shape memory properties of shape memory epoxy resin. *Mater. Sci. Eng. A* **2010**, *527*, 2510-2514.
136. Chiodo, J.D.; Billet, E.; Harrison, D. Active disassembly. *J. Sust. Des.* **1998**, 26-36.
137. Chiodo, J.D.; Harrison, D.J.; Billett, E.H. An initial investigation into active disassembly using shape memory polymers. *Proc. Inst. Mech. Eng. B J. Eng. Manu.* **2001**, *215*, 733-741.
138. Chiodo, J.D.; Boks, C. Assessment of end-of-life strategies with active disassembly using smart materials. *J. Sust. Prod. Des.* **2002**, *2*, 69-82.
139. Jefferson, A.; Joseph, C.; Lark, R.; Isaacs, B.; Dunn, S.; Weager, B. A new system for crack closure of cementitious materials using shrinkable polymers. *Cement Concrete Res.* **2010**, *50,* 795-801.
140. Ikeda, T.; Mamiya, J.-I.; Yu, Y. Photomechanics of liquid-crystalline elastomers and other polymers. *Angew. Chem. Int. Ed*. **2007**, *46*, 506-528.
141. Jana, R.N.; Yoo, H.J.; Cho, J.W. Synthesis and properties of shape memory polyurethane nanocomposites reinforced with poly(e-caprolactone)-grafted carbon nanotubes. *Fibers Polym.* **2008**, *9*, 247-254.
142. Sun, L.; Huang, W.M. Thermo/moisture responsive shape-memory polymer for possible surgery/operation inside living cells in future. *Mater. Des.* **2010**, *31*, 2684-2689.
143. Luo, X.; Lauber, K.E.; Mather, P.T. A thermally responsive, rigid, and reversible adhesive. *Polymer* **2010**, *51*, 1169-1175.
144. Wang, R.; Xie, T. Shape memory- and hydrogen bonding-based strong reversible adhesive system. *Langmuir* **2010**, *26*, 2999-3002.
145. Wischke, C.; Neffe, A.T.; Steuer, S.; Lendlein, A. Evaluation of a degradable shape-memory polymer network as matrix for controlled drug release. *J. Controlled Release* **2009**, *138*, 243-250.
146. Kimura, H.; Teraoka, F. Application of shape memory polymer to dental materials (part 1)—physical properties. *J. Osaka Univ. Dent. Sch.* **1986**, *26*, 59-65.
147. Nakasima, A.; Hu, J.R.; Ichinose, M.; Shimada, H. Potential application of shape memory plastic as elastic material in clinical orthodontics. *Eur. J. Orthod.* **1991**, *13*, 179-186.
148. Lendlein, A.; Langer, R. Biodegradable, elastic shape-memory polymers for potential biomedical applications. *Science* **2002**, *296*, 1673-1676.
149. Sokolowski, W.; M*etc*alfe, A.; Hayashi, S.; Yahia, L.; Raymond, J. Medical applications of shape memory polymers. *Biomed. Mater.* **2007**, *2*, S23-S27.

150. Nji, J.; Li, G. A self-healing 3D woven fabric reinforced shape memory polymer composite for impact mitigation. *Smart Mater. Struct*. **2010**, doi: 10.1088/0964-1726/19/3/035007.
151. Cho, T.K.; Chong, M.H.; Chun, B.C.; Kim, H.R.; Chung, Y.-C. Structure-property relationship and shape memory effect of polyurethane copolymer cross-linked with pentaerythritol. *Fibers Polym.* **2007**, *8*, 7-12.
152. Cho, J.W.; Jung, Y.C.; Chung, Y.-C.; Chun, B.C. Improved mechanical properties of shape-memory polyurethane block copolymers through the control of the soft-segment arrangement. *J. Appl. Polym. Sci.* **2004**, *93*, 2410-2415.
153. Lee, B.S.; Chun, B.C.; Chung, Y.-C.; Sul, K.I.; Cho, J.W. Structure and thermomechanical properties of polyurethane block copolymers with shape memory effect. *Macromolecules* **2001**, *34*, 6431-6437.
154. D'hollander, S.; Gommes, C.J.; Mens, R.; Adriaensens, P.; Goderis, B.; Du Prez, F. Modeling the morphology and mechanical behavior of shape memory polyurethanes based on solid-state NMR and synchrotron SAXS/WAXD. *J. Mater. Chem.* **2010**, *20*, 3475-3486.
155. Kim, B.K.; Lee, S.Y.; Lee, J.S.; Baek, S.H.; Choi, Y.J.; Lee, J.O.; Xu, M. Polyurethane ionomers having shape memory effects. *Polymer* **1998**, *39*, 2803-2808.
156. Jeong, H.M.; Ahn, B.K.; Kim, B.K. Temperature sensitive water vapour permeability and shape memory effect of polyurethane with crystalline reversible phase and hydrophilic segments. *Polym. Int.* **2000**, *49*, 1714-1721.
157. Yang, J.-E.; Kong, J.-S.; Park, S.-W.; Lee, D.-J.; Kim, H.-D. Preparation and properties of waterborne polyurethane-urea anionomers. I. The influence of the degree of neutralization and counterion. *J. Appl. Polym. Sci.* **2002**, *86*, 2375-2383.
158. Zhu, Y.; Hu, J.; Yeung, K. Effect of soft segment crystallization and hard segment physical crosslink on shape memory function in antibacterial segmented polyurethane ionomers. *Acta Biomater.* **2009**, *5*, 3346-3357.
159. Chen, S.; Cao, Q.; Jing, B.; Cai, Y.; Liu, P.; Hu, J. Effect of microphase-separation promoters on the shape-memory behavior of polyurethane. *J. Appl. Polym. Sci.* **2006**, *102*, 5224-5231.
160. Cao, Q.; Liu, P. Structure and mechanical properties of shape memory polyurethane based on hyperbranched polyesters. *Polym. Bull.* **2006**, *57*, 889-899.
161. Yates, C.R.; Hayes, W. Synthesis and applications of hyperbranched polymers. *Eur. Polym. J.* **2004**, *40*, 1257-1281.
162. Voit, B.I.; Lederer, A. Hyperbranched and highly branched polymer architectures—Synthetic strategies and major characterization aspects. *Chem. Rev.* **2009**, *109*, 5924-5973.
163. Sivakumar, C.; Nasar, A.S. Poly(ε-caprolactone)-based hyperbranched polyurethanes prepared via A2 + B3 approach and its shape-memory behavior. *Eur. Polym. J.* **2009**, *45*, 2329-2337.
164. Behl, M.; Lendlein, A. Shape-memory polymers. *Mater. Today* **2007**, *10*, 20-28.
165. Zeng, M.; Zhang, L. Effects of reaction and cure temperatures on morphology and properties of poly(ester-urethane). *J. Appl. Polym. Sci.* **2006**, *100*, 708-714.
166. Zeng, M.; Zhang, D. Effects of temperature on morphology and properties of films prepared from poly(ester-urethane) and nitrochitosan. *Macromol. Mater. Eng.* **2006**, *291*, 148-154.
167. Hu, J.L.; Zeng, Y.M.; Yan, H.J. Influence of processing conditions on the microstructure and properties of shape memory polyurethane membranes. *Text. Res. J.* **2003**, *73*, 172-178.

168. Ji, F.L.; Zhu, Y.; Hu, J.L.; Liu, Y.; Yeung, L.-Y.; Ye, G.D. Smart polymer fibers with shape memory effect. *Smart Mater. Struct.* **2006**, *15*, 1547-1554.
169. Zhuo, H.; Hu, J.; Chen, S. Electrospun polyurethane nanofibres having shape memory effect. *Mater. Lett.* **2008**, *62*, 2074-2076.
170. Han, J.; Chen, B.; Ye, L.; Zhang, A.-Y.; Zhang, J.; Feng, Z.-G. Synthesis and characterization of biodegradable polyurethane based on poly(ε-caprolactone) and L-lysine ethyl ester diisocyanate. *Front. Mater. Sci. China* **2009**, *3*, 25-32.
171. Mondal, S.; Hu, J.L. Structural characterization and mass transfer properties of nonporous-segmented polyurethane membrane: Influence of the hydrophilic segment content and soft segment melting temperature. *J. Membr. Sci.* **2006**, *276*, 16-22.
172. Mondal, S.; Hu, J.L. A Novel Approach to excellent uv protecting cotton fabric with functionalized MWNT Containing water vapor permeable PU coating. *J. Appl. Polym. Sci.* **2007**, *103*, 3370-3376.
173. Jeong, H.M.; Ahn, B.K.; Cho, S.M.; Kim, B.K. Water vapor permeability of shape memory polyurethane with amorphous reversible phase. *J. Polym. Sci. Part B Polym. Phys.* **2000**, *38*, 3009-3017.
174. Lin, J.R.; Chen, C.-Y. Study on Shape-memory behavior of polyether-based polyurethanes. I. Influence of the hard-segment content. *J. Appl. Polym. Sci.* **1998**, *69*, 1563-1574.
175. Lin, J.R.; Chen, L.W. Study on shape-memory behavior of polyether-based polyurethanes. II. Influence of soft-segment molecular weight. *J. Appl. Polym. Sci.* **1998**, *69*, 1575-1586.
176. Liu, G.; Ding, X.; Cao, Y.; Zheng, Z.; Peng, Y. Shape memory of hydrogen-bonded polymer network/poly(ethyleneglycol) complexes. *Macromolecules* **2004**, *37*, 2228-2232.
177. Atli, B.; Gandhi, F.; Kars, G. Thermomechanical characterization of shape memory polymers. *J. Intell. Mater. Sys. Struct.* **2009**, *20*, 87-89.
178. Qi, H.J.; Nguyen, T.D.; Castro, F.; Yakacki, C.M.; Shandas, R. Finite deformation thermo-mechanical behavior of thermally induced shape memory polymers. *J. Mech. Phys. Solids.* **2008**, *56*, 1730-1751.
179. Tobushi, H.; Matsui, R.; Hayashi, S.; Shimada, D. The influence of shape-holding conditions on shape recovery of polyurethane-shape memory polymer foams. *Smart Mater. Struct.* **2004**, *13*, 881-887.
180. Huang, W.M.; Lee, C.W.; Teo, H.P. Thermomechanical behavior of a polyurethane shape memory polymer foam. *J. Intell. Mater. Sys. Struct.* **2006**, *17*, 753-760.
181. Li, G.; Nettles, D. Thermomechanical characterization of a shape memory polymer based self-repairing syntactic foam. *Polymer* **2010**, *51*, 755-762.
182. Domeier, L.; Nissen, A.; Goods, S.; Whinnery, L.; McElhanon, J. Thermomechanical characterization of thermoset urethane shape-memory polymer foams. *J. Appl. Polym. Sci.* **2010**, *115*, 3217-3229.
183. Di Prima, M.A.; Gall, K.; McDowell, D.L.; Guldberg, R.; Lin, A.; Sanderson, T.; Campbell, D.; Arzberger, S.C. Cyclic compression behavior of epoxy shape memory polymer foam. *Mech. Mater.* **2010**, *42*, 405-416.
184. Liu, C.; Mather, P.T. Thermomechanical characterization of a tailored series of shape memory polymers. *J. Appl. Med. Polym.* **2002**, *6*, 47-52.

185. Liu, C.; Mather, P.T. Thermomechanical characterization of blends of poly(vinyl acetate) with semicrystalline polymers for shape memory applications. *ANTEC Conf. Proc.* **2003**, 1962-1966.
186. Gunes, I.S.; Cao, F.; Jana, S.C. Effect of thermal expansion on shape memory behavior of polyurethane and its nanocomposites. *J. Polym. Sci. B Polym. Phys.* **2008**, *46*, 1437-1449.
187. Yakacki, C.M.; Willis, S.; Luders, C.; Gall, K. Deformation Limits in shape-memory polymers. *Adv. Eng. Mater.* **2008**, *10*, 112-119.
188. Liu, Y.; Gall, A.; Dunn, M.L.; McCluskey, P. Thermomechanical recovery couplings of shape memory polymers in flexure. *Smart Mater. Struct.* **2003**, *12*, 947-954.
189. Miaudet, P.; Derré, A.; Maugey, M.; Zakri, C.; Piccione, P.M.; Inoubli, R.; Poulin, P. Shape and Temperature memory of nanocomposites with broadened glass transition. *Science* **2007**, *318*, 1294-1296.
190. Liang, C.; Rogers, C.A.; Malafeew, E. Investigation of shape memory polymers and their hybrid composites. *J. Intell. Mater. Sys. Struct.* **1997**, *8*, 380-386.
191. Ohki, T.; Ni, Q.-Q.; Ohsako, N.; Iwamoto, M. Mechanical and shape memory behavior of composites with shape memory polymer. *Compos. A* **2004**, *35*, 1065-1073.
192. Viry, L.; Mercader, C.; Miaudet, P.; Zakri, C.; Derré, A.; Kuhn, A.; Maugey, M.; Poulin, P. Nanotube fibers for electromechanical and shape memory actuators. *J. Mater. Chem.* **2010**, *20*, 3487-3495.
193. Xu, B.; Fu, Y.Q.; Ahmad, M.; Luo, J.K.; Huang, W.M.; Kraft, A.; Reuben, R.; Pei, Y.T.; Chen, Z.G.; De Hosson, J.T.M. Thermo-mechanical properties of polystyrene-based shape memory nanocomposites. *J. Mater. Chem.* **2010**, *20*, 3442-3448.
194. Jung, D.H.; Jeong, H.M.; Kim, B.K. Organic-inorganic chemical hybrids having shape memory effect. *J. Mater. Chem.* **2010**, *20*, 3458-3466.
195. Mondal, S.; Hu, J.L. Shape memory studies of functionalized mwnt-reinforced polyurethane copolymers. *Iran. Polym. J.* **2006**, *15*, 135-142.
196. Koerner, H.; Price, G.; Pearce, N.A.; Alexander, M.; Vaia, R.A. Remotely actuated polymer nanocomposites—Stress-recovery of carbon-nanotube-filled thermoplastic elastomers. *Nat. Mater.* **2004**, *3*, 115-120.
197. Deka, H.; Karak, N.; Kalita, R.D.; Buragohain, A.K. Biocompatible hyperbranched polyurethane/multi-walled carbon nanotube composites as shape memory materials. *Carbon* **2010**, *48*, 2013-2022.
198. Gunes, I.S.; Cao, F.; Jana, S.C. Evaluation of nanoparticulate fillers for development of shape memory polyurethane nanocomposites. *Polymer* **2008**, *49*, 2223-2234.
199. Razzaq, M.Y.; Frormann, L. Thermomechanical studies of aluminum nitride filled shape memory polymer composites. *Polym. Compos.* **2007**, *28*, 287-293.
200. Zhang, S.; Yu, Z.; Govender, T.; Luo, H.; Li, B. A novel supramolecular shape memory material based on partial α-CD-PEG inclusion complex. *Polymer* **2008**, *49*, 3205-3210.
201. Gall, K.; Dunn, M.L.; Liu, Y.; Finch, D.; Lake, M.; Munshi, N.A. Shape memory polymer nanocomposites. *Acta. Mater.* **2002**, *50*, 5115-5126.
202. Ohki, T.; Ni, Q.-Q.; Iwamoto, M. Creep and cyclic mechanical properties of composites based on shape memory polymer. *Sci. Eng. Compos. Mater.* **2004**, *11*, 137-147.

203. Cao, F.; Jana, S.C. Nanoclay-tethered shape memory polyurethane nanocomposites. *Polymer* **2007**, *48*, 3790-3800.
204. Zhang, C.-S.; Ni, Q.-Q.; Fu, S.-Y.; Kurashiki, K. Electromagnetic interference shielding effect of nanocomposites with carbon nanotube and shape memory polymer. *Compos. Sci. Technol.* **2007**, *67*, 2973-2980.
205. Sahoo, N.G.; Jung, Y.C.; Yoo, H.J.; Cho, J.W. Influence of carbon nanotubes and polypyrrole on the thermal, mechanical and electroactive shape-memory properties of polyurethane nanocomposites. *Compos. Sci. Technol.* **2007**, *67*, 1920-1929.
206. Jung, Y.C.; Goo, N.S.; Cho, J.W. Electrically conducting shape memory polymer composites for electroactive actuator. *Proc. SPIE* **2004**, *5385*, 230-234.
207. Leng, J.; Lv, H.; Liu, Y.; Du, S. Synergic effect of carbon black and short carbon fiber on shape memory polymer actuation by electricity. *J. Appl. Phys.* **2008**, doi: 10.1063/1.3026724.
208. Leng, J.; Lan, X.; Liu, Y.; Du, S. Electroactive thermoset shape memory polymer nanocomposite filled with nanocarbon powders. *Smart. Mater. Struct.* **2009**, doi: 10.1088/0964-1726/18/7/074003.
209. Sahoo, N.G.; Jung, Y.C.; Goo, N.S.; Cho, J.W. Conducting shape memory polyurethane-polypyrrole composites for an electroactive actuator. *Macromol. Mater. Eng.* **2005**, *290*, 1049-1055.
210. Lu, H.; Liu, Y.; Gou, J.; Leng, J.; Du, S. Synergistic effect of carbon nanofiber and carbon nanopaper on shape memory polymer composite. *Appl. Phys. Lett.* **2010**, doi: 10.1063/1.3323096.
211. Madbouly, S.A.; Lendlein, A. Shape-memory polymer composites. In *Advances in Polymer Science*; Springer: Berlin, Germany, 2009; Volume 226, pp. 41-95.
212. Weigel, T.; Mohr, R.; Lendlein, A. Investigation of parameters to achieve temperatures required to initiate the shape-memory effect of magnetic nanocomposites by inductive heating. *Smart Mater. Struct.* **2009**, doi: 10.1088/0964-1726/18/2/025011.
213. Schmidt, A.M. Thermoresponsive magnetic colloids. *Colloid. Polym. Sci.* **2007**, *285*, 953-966.
214. Yakacki, C.M.; Satarkar, N.S.; Gall, K.; Likos, R.; Hilt, J.Z. Shape-Memory Polymer Networks with Fe3O4 Nanoparticles for Remote Activation. *J. Appl. Polym. Sci.* **2009**, *112*, 3166-3176.
215. Kumar, U.N.; Kratz, K.; Wagermaier, W.; Behl, M.; Lendlein, A. Non-contact actuation of triple-shape effect in multiphase polymer network nanocomposites in alternating magnetic field. *J. Mater. Chem.* **2010**, *20*, 3404-3415.
216. Jordan, A.; Scholz, R.; Wust, P.; Fahling, H.; Felix, R. Magnetic fluid hyperthermia (MFH): Cancer treatment with AC magnetic field induced excitation of biocompatible superparamagnetic nanoparticles. *J. Magn. Magn. Mater.* **1999**, *201*, 413-419.
217. Yang, B.; Huang, W.M.; Li, C.; Lee, C.M.; Li, L. On the effects of moisture in a polyurethane shape memory polymer. *Smart Mater. Struct*. **2004**, *13*, 191-195.
218. Yang, B.; Huang, W.M.; Li, C.; Chor, J.H. Effects of moisture on the glass transition temperature of polyurethane shape memory polymer filled with nano-carbon powder. *Eur. Polym. J.* **2005**, *41*, 1123-1128.
219. Du, H.; Zhang, J. Shape memory polymer based on chemically cross-linked poly(vinyl alcohol) containing a small number of water molecules. *Colloid. Polym. Sci.* **2010**, *288*, 15-24.

220. Jung, Y.C.; So, H.H.; Cho, J.W. Water-responsive shape memory polyurethane block copolymer modified with polyhedral oligomeric silsesquioxane. *J. Macrom. Sci. Part B Phys.* **2006**, *45*, 453-461.
221. Lu, H.; Liu, Y.; Leng, J.; Du, S. Qualitative separation of the effect of the solubility parameter on the recovery behavior of shape-memory polymer. *Smart Mater. Struct.* **2009**, doi: 10.1088/0964-1726/18/8/085003.
222. Mark, J.E.; Erman, B. *Rubberlike Elasticity-A: Molecular Primer*; Cambridge University Press: New York, NY, USA, 1988.
223. Gunes, I.S.; Jana, S.C. Shape Memory Polymers and Their Nanocomposites: A review of science and technology of new multifunctional materials. *J. Nanosci. Nanotech.* **2008**, *8*, 1616-1637.
224. Hayashi, S. *Technical Report on Shape Memory Polymers*; Nagoya Research and Development Center, Mitsubishi Heavy Industries, Inc.: Nagoya, Japan, 1990.
225. Müller, W.; Pretsch, T. Hydrolytic aging of crystallizable shape memory poly(ester urethane): Effects on the thermo-mechanical properties and visco-elastic modeling. *Eur. Polym. J.* **2010**, *46*, 1745-1758.
226. Pretsch, T. *Degradation, Functional Stability and Protection of a Shape Memory Polymer*; WMRIF Workshop for young scientists: Tsukuba, Japan, 2008; XXX-1-11; Available online: http://www.bam.de/de/kompetenzen/fachabteilungen/abteilung_4/fg43/fg43_medien/div43_ag2_article_pretsch_japan_2008.pdf (accessed on 21 July 2010).
227. Pretsch, T.; Jakob, I.; Müller, W. Hydrolytic degradation and functional stability of a segmented shape memory poly(ester urethane). *Polym. Degradation Stability* **2009**, *94*, 61-73.
228. Pretsch, T.; Müller, W. Shape memory poly(ester urethane) with improved hydrolytic stability. *Polym. Degrad. Stab.* **2010**, *95*, 880-888.
229. Pretsch, T. Durability of a polymer with triple-shape properties. **2010**, submitted.
230. Tandon, G.P.; Goecke, K.; Cable, K.; Baur, J. Durability assessment of styrene- and epoxy-based shape-memory polymer resins. *J. Intell. Mater. Sys. Struct.* **2009**, *20*, 2127-2143.
231. Meents, E.P.; Barnell, T.J.; Cable, K.M.; Margraf, T.W.; Havens, E. Self-healing reflexive composite structures for marine environments. In *Proceedings of SAMPE 2009*, Baltimore, MD, USA, 18–21 May 2009.
232. Zheng, X.; Zhou, S.; Yu, X.; Li, X.; Feng, B.; Qu, S.; Weng, J. Effect of *in vitro* degradation of poly(d,l-lactide)/b-tricalcium composite on its shape-memory properties. *J. Biomed. Mater. Res. B Appl. Biomater.* **2008**, *86B*, 170-180.
233. Yu, X.; Zhou, S.; Zheng, X.; Xiao, Y.; Guo, T. Influence of *in vitro* degradation of a biodegradable nanocomposite on its shape memory effect. *J. Phys. Chem. C* **2009**, *113*, 17630-17635.
234. Zhang, D.; Liu, Y.; Leng, J. Influence of radiation dose on shape memory effect of styrene copolymer. *Proc. SPIE* **2009**, doi:10.1117/12.815696.
235. Yang, W.P.; Macosko, C.W.; Wellinghoff, S.T. Thermal degradation of urethanes based on 4,4′-diphenylmethane diisocyanate and 1,4-butanediol (MDI/BDO). *Polymer* **1986**, *27*, 1235-1240.
236. Petrovic, Z.S.; Zavargo, Z.; Flyn, J.H.; Macknight, W.J. Thermal degradation of segmented polyurethanes. *J. Appl. Polym. Sci.* **1994**, *54*, 1087-1095.

237. Razzaq, M.Y.; Anhalt, M.; Frormann, L.; Weidenfeller, B. Mechanical spectroscopy of magnetite filled polyurethane shape memory polymers. *Mater. Sci. Eng. A* **2007**, *471*, 57-62.
238. Jana, R.N.; Cho, J.W. Thermal stability and molecular interaction of polyurethane nanocomposites prepared by *in situ* polymerization with functionalized multiwalled carbon nanotubes. *J. Appl. Polym. Sci.* **2008**, *108*, 2857-2864.
239. Schmidt, C.; Neuking, K.; Eggeler, G. Functional fatigue of shape memory polymers. *Adv. Eng. Mater.* **2008**, *10*, 922-927.
240. Schmidt, C.; Neuking, K.; Eggeler, G. Functional fatigue of shape-memory polymers. *Mater. Res. Soc. Symp. Proc.* **2009**, *1190*, 43-48.
241. M*etc*alfe, A.; Desfaits, A.-C.; Salazkin, I.; Yahia, L.H.; Sokolowski, W.M.; Raymond, J. Cold hibernated elastic memory foams for endovascular interventions. *Biomaterials* **2003**, *24*, 491-497.
242. Wang, W.; Ping, P.; Chen, X.; Jing, X. Biodegradable polyurethane based on random copolymer of l-lactide and e-caprolactone and its shape-memory property. *J. Appl. Polym. Sci*. **2007**, *104*, 4182-4187.
243. Choi, N.-Y.; Kelch, S.; Lendlein, A. Synthesis. Shape-memory functionality and hydrolytical degradation studies on polymer networks from poly(rac-lactide)-b-poly(propylene oxide)-b-poly(rac-lactide)dimethacrylates. *Adv. Eng. Mater.* **2006**, *8*, 439-445.
244. Ping, P.; Wang, W.; Chen, X.; Jing, X. Poly(caprolactone) polyurethane and its shape-memory property. *Biomacromolecules* **2005**, *6*, 587-592.
245. Alteheld, A.; Feng, Y.; Kelch, S.; Lendlein, A. Biodegradable, amorphous copolyester-urethane networks having shape-memory properties. *Angew .Chem. Int. Ed.* **2005**, *44*, 1188-1192.
246. Venkatraman, S.S.; Tan, L.P.; Joso, J.F.D.; Boey, Y.C.F.; Wang, X. Biodegradable stents with elastic memory. *Biomacromolecules* **2006**, *27*, 1573-1578.
247. Zini, E.; Scandola, M.; Dobrzynski, P.; Kasperczyk, J.; Bero, M. Shape Memory behavior of novel (l-lactide-glycolide-trimethylene carbonate) terpolymers. *Biomacromolecules* **2007**, *8*, 3661-3667.
248. Luo, H.; Liu, Y.; Yu, Z.; Zhang, S.; Li, B. Novel biodegradable shape memory material based on partial inclusion complex formation between α-cyclodextrin and poly(ε-caprolactone). *Biomacromolecules* **2008**, *9*, 2573-2577.
249. Knight, P.T.; Lee, K.M.; Qin, H.; Mather, P.T. Biodegradable thermoplastic polyurethanes incorporating polyhedral oligosilsesquioxane. *Biomacromolecules* **2008**, *9*, 2458-2467.
250. Wang, L.-S.; Chen, H.-C.; Xiong, Z.-C.; Pang, X.-B.; Xiong, C.-D. Novel degradable compound shape-memory-polymer blend: Mechanical and shape-memory properties. *Mater. Lett.* **2010**, *64*, 284-286.
251. Gautrot, J.E.; Zhu, X.X. Shape memory polymers based on naturally-occurring bile acids. *Macromolecules* **2009**, *42*, 7324-7331.
252. Thérien-Aubin, H.; Gautrot, J.E.; Shao, Y.; Zhang, J.; Zhu, X.X. Shape memory properties of main chain bile acids polymers. *Polymer* **2010**, *51*, 22-25.
253. Liu, L.; Cai, W. Novel copolyester for a shape-memory biodegradable material *in vivo*. *Mater. Lett.* **2009**, *63*, 1656-1658.

254. Migneco, F.; Huang, Y.-C.; Birla, R.K.; Hollister, S.J. Poly(glycerol-dodecanoate), a biodegradable polyester for medical devices and tissue engineering scaffolds. *Biomaterials* **2009**, *30*, 6479-6484.
255. Nagahama, K.; Ueda, Y.; Ouchi, T.; Ohya, Y. Biodegradable shape-memory polymers exhibiting sharp thermal transitions and controlled drug release. *Biomacromolecules* **2009**, *10*, 1789-1794.
256. Xue, L.; Dai, S.; Li, Z. Synthesis and characterization of three-arm poly(ε-caprolactone)-based poly(ester urethanes) with shape-memory effect at body temperature. *Macromolecules* **2009**, *42*, 964-972.
257. Wang, Y.; Li, Y.; Luo, Y.; Huang, M.; Liang, Z. Synthesis and characterization of a novel biodegradable thermoplastic shape memory polymer. *Mater. Lett.* **2009**, *63*, 347-349.
258. Small, W.; Singhal, P.; Wilson, T.S.; Maitland, D.J. Biomedical applications of thermally activated shape memory polymers. *J. Mater. Chem.* **2010**, *20*, 3356-3366.
259. Lendlein, A.; Behl, M.; Hiebl, B.; Wischke, C. Shape-memory polymers as a technology platform for biomedical applications. *Expert Rev. Med. Devices* **2010**, *7*, 357-379.
260. Wischke, C.; Lendlein, A. Shape-memory polymers as drug carriers—A multifunctional system. *Pharm. Res.* **2010**, *27*, 527-529.
261. Neuss, S.; Blomenkamp, I.; Stainforth, R.; Boltersdorf, D.; Jansen, M.; Butz, N.; Perez-Bouza, A.; Knüchel, R. The use of a shape-memory poly(ε{lunate}-caprolactone)dimethacrylate network as a tissue engineering scaffold. *Biomaterials* **2009**, *30*, 1697-1705.
262. Ortega, J.M.; Small, W.; Wilson, T.S.; Benett, W.J.; Loge, J.M.; Maitland, D.J. A shape memory polymer dialysis needle adapter for the reduction of hemodynamic stress within arteriovenous grafts. *IEEE Trans. Biomed. Eng.* **2007**, *54*, 1722-1724.
263. Lorenzo, V.; Díaz-Lantada, A.; Lafont, P.; Lorenzo-Yustos, H.; Fonseca, C.; Acosta, J. Physical ageing of a PU-based shape memory polymer: Influence on their applicability to the development of medical devices. *Mater. Des.* **2009**, *30*, 2431-2434.
264. Farè, S.; De Nardo, L.; De Cicco, S.; Jovenitti, M.; Tanzi, M.C. Different processing methods to obtain porous structure in shape memory polymers. *Mater. Sci*. *Forum* **2007**, *539-543*, 663-668.
265. Yang, J.; Liu, F.; Yang, L.; Li, S. Hydrolytic and enzymatic degradation of poly(trimethylene carbonate-co-d,l-lactide) random copolymers with shape memory behavior. *Eur. Polym. J.* **2010**, *46*, 783-791.
266. Wache, M.; Tartakowska, J.; Hentrich, A.; Wagner, M. Development of a polymer stent with shape memory effect as a drug delivery system. *J. Mater. Sci. Mater Med.* **2003**, *14*, 109-112.
267. Kim, J.H.; Kang, T.J.; Yu, W.-R. Simulation of mechanical behavior of temperature-responsive braided stents made of shape memory polyurethanes. *J. Biomech.* **2010**, *43*, 632-643.
268. Sharp, A.A.; Panchawagh, H.V.; Ortega, A.; Artale, R.; Richardson-Burns, S.; Finch, D.S.; Gall, K.; Mahajan, R.L.; Restrepo, D. Toward a self-deploying shape memory polymer neuronal electrode. *J. Neural. Eng.* **2006**, *3*, L23-L30.
269. Huang, W.M. Thermo-moisture responsive polyurethane shape memory polymer for biomedical devices. *Open Med. Devices J.* **2010**, *2*, 11-19.
270. Nelson, G.R. Expansible polyurethane foam. U.S. Patent 3,284,275, 8 November 1966.

271. Di Prima, M.A.; Lesniewski, M.; Gall, K.; McDowell, D.L.; Sanderson, T.; Campbell, D. Thermo-mechanical behavior of epoxy shape memory polymer foams. *Smart Mater. Struct.* **2007**, *16*, 2330-2340.
272. Simkevitz, S.L.; Naguib, H.E. Fabrication and analysis of porous shape memory polymer and nanocomposites. *High Perform. Polym.* **2010**, *22*, 159-183.
273. Ortega, J.; Maitland, D.; Wilson, T.; Tsai, W.; Savas, Ö.; Saloner, D. Vascular dynamics of a shape memory polymer foam aneurysm treatment technique. *Ann. Biomed. Eng.* **2007**, *35*, 1870-1884.
274. Small, W.; Buckley, P.R.; Wilson, T.S.; Benett, W.J.; Hartman, J.; Saloner, D.; Maitland, D.J. Shape memory polymer stent with expandable foam: A new concept for endovascular embolization of fusiform aneurysms. *IEEE Trans. Biomed. Eng.* **2007**, *54*, 1157-1160.
275. Vialle, G.; Prima, M.A.D.; Hocking, E.; Gall, K.; Garmestani, H.; Sanderson, T.; Arzberger, S.; Campbell, D. Remote activation of nanomagnetite reinforced shape memory polymer foam. *Smart Mater. Struct.* **2009**, doi: 10.1088/0964-1726/18/11/115014.
276. Di Prima, M.; Gall, K.; McDowell, D.L.; Guldberg, R.; Lin, A.; Sanderson, T.; Campbell, D.; Arzberger, S.C. Deformation of epoxy shape memory polymer foam. Part I: Experiments and macroscale constitutive modeling. *Mech. Mat.* **2010**, *42*, 304-314.
277. Tey, S.J.; Huang, W.M.; Sokolowski, W. Influence of long-term storage in cold hibernation on strain recovery and recovery stress of polyurethane shape memory polymer foam. *Smart Mater. Struct.* **2001**, *10*, 321-325.
278. Di Prima, M.A.; Gall, K.; McDowell, D.L.; Guldberg, R.; Lin, A.; Sanderson, T.; Campbell, D.; Arzberger, S.C. Deformation of epoxy shape memory polymer foam: Part II. Mesoscale modeling and simulation. *Mech. Mater.* **2010**, *42*, 315-325.
279. White, S.R.; Sottos, N.R.; Geubelle, P.H.; Moore, J.S.; Kessler, M.R.; Sriram, S.R.; Brown, E.N.; Viswanathan, S. Autonomic healing of polymer composites. *Nature* **2001**, *409*, 794-797.
280. Blaiszik, B.J.; Sottos, N.R.; White, S.R. Nanocapsules for self-healing materials. *Compos. Sci. Tech.* **2008**, *68*, 978-986.
281. Pang, J.W.C.; Bond, I.P. A hollow fibre reinforced polymer composite encompassing self-healing and enhanced damage visibility. *Compos. Sci. Tech.* **2005**, *65*, 1791-1799.
282. Li, G.; John, M. A self-healing smart syntactic foam under multiple impacts. *Compos. Sci. Technol.* **2008**, *68*, 3337-3343.